UNIVERSITY OF CALGARY

Business Case for Geothermal Energy Development to power LNG Project in BC

by

Yaqub Olabanji Adepoju

A RESEARCH PROJECT SUBMITTED

IN PARTIAL FULFILMENT OF THE REQUIREMENTS FOR THE

DEGREE OF MASTER OF SCIENCE

GRADUATE PROGRAM IN SUSTAINABLE ENERGY DEVELOPMENT

CALGARY, ALBERTA

AUGUST, 2020

Abstract

Geological uncertainties of the Mount Meager volcanic complex in British Columbia, Canada, are analyzed to evaluate the economic viability of a geothermal power plant. This study utilizes empirical petrophysical formulas combined with field data to estimate geologic properties, including rock porosity and permeability. Flow rate, outlet pressure and temperature for three different conceptual flow models, two types of closed loop systems and one open loop system, were simulated. An economic analysis was carried out to understand the impact of rock permeability uncertainty and geothermal aquifer temperature on technical feasibility and economics viability of a geothermal power plant the complex. This study found that Enhanced Geothermal System (EGS) implementation can deliver a mass flow rate of up to 63kg/sec of 197^{o}C fluid from the subsurface in the study area. Sensitivity analyses suggests that permeability is critical for the project economics. De-risking rock permeability with further research and reducing well costs will improve the economic viability of geothermal resource development in British Columbia and should be pursued further.

Table of Contents

List of Tables

List of Figures

List of Abbreviation

BC	British Columbia
CF	Capacity Factor
EGS	Enhanced Geothermal Systems
GHG	Greenhouse Gas
GW	Gigawatt
kW	Kilowatt
kWh	Kilowatt-hour
LCOE	Levelized Cost of Energy
LNG	Liquified Natural Gas
MC	Meager Creek
MMVC	Mount Meager Volcanic complex
NPV	Net Present Value
NOX	Oxides of nitrogen, especially as atmospheric pollutants
FCF	Pan-Canadian Framework
UNFC	United Nations Framework Classification for Resources

Chapter 1 - Introduction

Canada is yet to contribute significantly to global geothermal electricity generation, which currently has a total installed capacity of 15.4 GW (Richter, 2020), primarily due to the economic advantage of cheaper alternatives in areas favorable to geothermal development. However, the need to grow this additional renewable energy is highlighted by the ongoing development of large industrial complexes, such as LNG Canada in Kitimat, BC, and other energy demanding economic developments. This project reviews previous works, and takes a qualitative approach to understand the uncertainties that is inherent in the exploitation of the geothermal resources in BC with focus on the aspects of the rock properties uncertainties which we believe has prevented developers from maturing the geothermal prospects identified over half a century ago.

A mixed research method was adopted, combining a review of available literature with basic quantitative analysis of available well and geologic data, to determine uncertainty that prevents a deterministic approach to estimating geothermal resource potentials in the region. Also, information obtained from interviews is also embedded and the results are benchmarked with available global data.

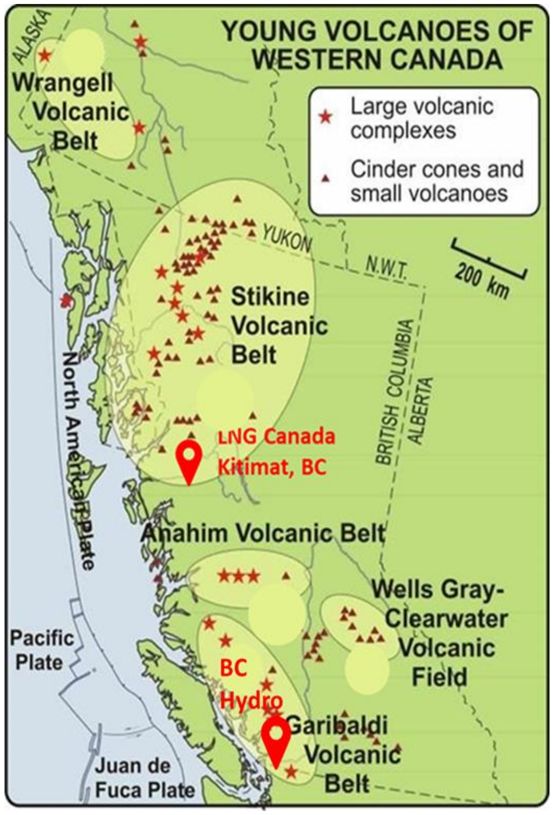

Figure 1: Map showing volcanic belts in Western Canadian (adopted from Natural Resources Canada, 2018)

The research question therefore states: “what economic scenario will make good business case for implementation of geothermal power industries situated along the western coast of Canada”. To address this research question, a section of the Mount Meager Volcanic Complex was selected as the study area, because of availability of required technical data and other information that can facilitate my analysis. Mount Meager Volcanic Complex is a group of volcanic peaks in the Pacific Ranges of the Coast Mountains in southwestern British Columbia. The study is located 150 km north of Vancouver at the northern end of the Pemberton Valley and reaches a maximum elevation of 2,680 m.

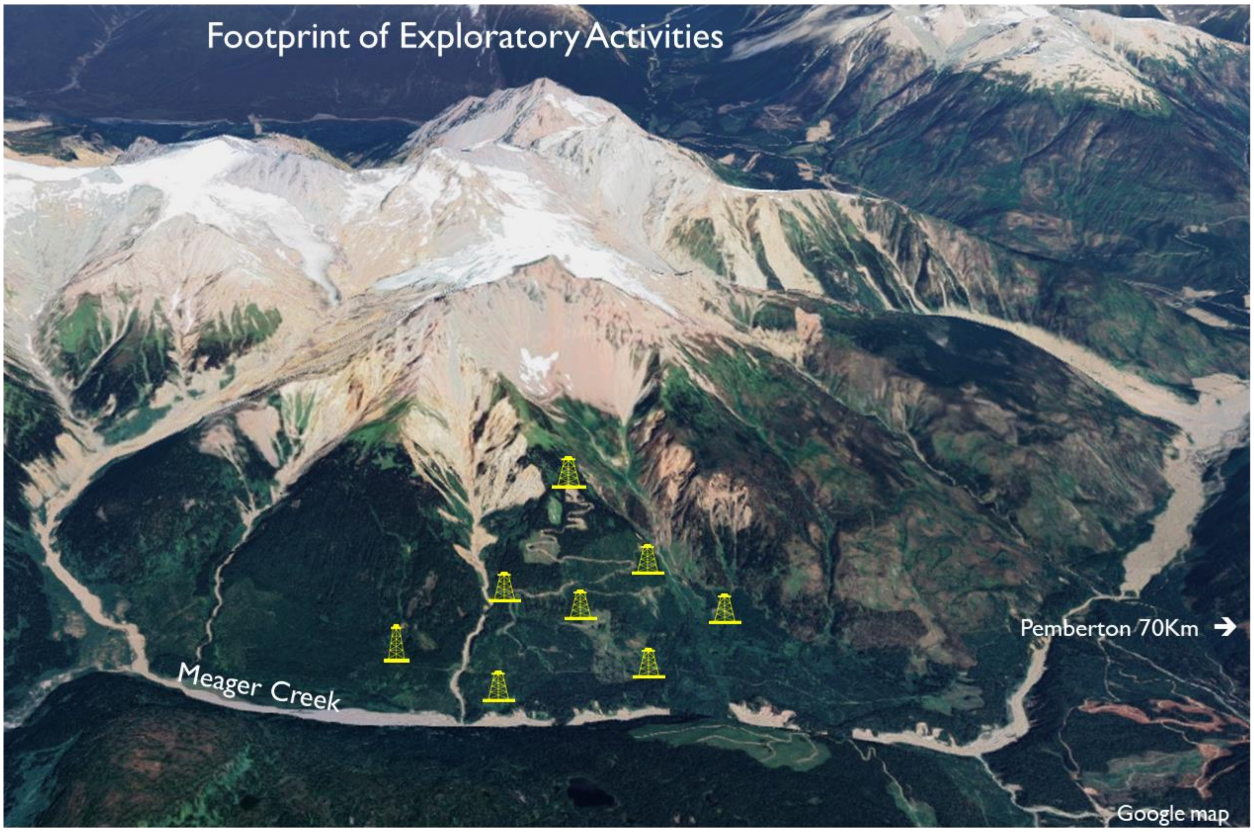

Figure 2: Google Earth view of Mount Meager, Squamish-Lillooet Creek, BC.

The region is uniquely positioned for commercial marine cargo opportunities. Apart from LNG Canada project, which is currently active, there are four proposed LNG plants. These proposed LNG plants are to be located at Kitimat, Tilbury and Woodfibre, while the fourth being proposed propane export terminal to be located at Ridley Island, Prince Rupert, BC. LNG Canada is a large industrial energy project that will build and operate a terminal for the liquefaction, storage, and loading of liquefied natural gas in the port of Kitimat, in the traditional territory of the Haisla Nation, British Columbia, Canada. It will export LNG produced by the project's partners in the Montney Formation gas fields near Dawson Creek, B.C. LNG Canada is a joint venture company comprised of Shell Canada Energy, and Petronas; an affiliate of PetroChina, Mitsubishi

Corporation, and Korea Gas Corporation. Final investment decision was taken in 2018 and construction work is well underway.

Figure 3: A visual representation of LNG projects in B.C. and the proposed current export facilities and pipelines map.

"LNG Canada will export Canadian natural gas to Asian markets, and in the process, put Canada on the global map of LNG exporting countries and create a world-class liquefied natural gas (LNG) industry in British Columbia and Canada" (LNG Canada, 2020).

In terms of electricity power, the main Liquefication compression facility which is 80% of required electricity for the entire plant is planned to be powered by natural gas while remaining 20% will be sourced from BC Hydro power, which is renewable, only for the ancillary services. However, according to Clean Energy Canada, the 2018 Climate Action in BC, which was set to achieve an 80% GHG reduction by 2050, will be difficult to achieve if any large LNG plants is powered mostly or completely by natural gas. It was observed by the same agency, that any BC LNG proponent that chooses to maximize use of renewable energy in its facility will create 45% more permanent local jobs, 33% less carbon emission and pollution (Glave & Moorhouse, 2014). "Adding up the emissions from liquefying the gas and all the upstream emissions from production, LNG Canada represents roughly 10 million tonnes of CO2-equivalent per year. This is one quarter of B.C.'s entire greenhouse-gas budget for 2030, or two-thirds of B.C.'s 2050 target" (Shaffer, 2018).

1.1 Socio-Economic and Environmental Dimensions of Geothermal Energy in BC

Sustainable energy systems are crucial to all three dimensions of sustainable development and thus central for mitigating climate change and achieving sustainable economic and social development. (Lechtenböhmer & Nilsson, 2016). Geothermal energy is a sustainable energy that can be available for as long as the Earth exist. Even though geothermal especially from natural hot springs has been used for centuries to meet various heating needs ranging from cooking to bathing, it was not until 1904 that the first application of it for electricity general came about. DiPippo 2016 stated that in 1904, Prince P. G. Conti set up the first device that was able to produce electricity from a geothermal steam well. Ten years later, in 1914, at the same location, a 250-kW turbo-alternator was the first commercial geothermal power system connected to the grid. Ever since, the geothermal energy exploitation blossoms. The installed capacity of geothermal energy has gradually increased worldwide over the last decade, reaching 13.93 gigawatts in 2019 (Wang, 2020). Owing to its environmentally friendly nature, geothermal technologies are among the growing renewable energy trend occurring across the world. It is now being sought after because of reduced emissions and its renewable source. The renewable energy resource can also provide source of livelihood for local communities in and around the area it is located. Usually, geothermal resource occurs in environmentally sensitive areas of the world as it is indeed the case with the western coast of Canada. The Mount Meager Volcanic Complex in known for its instability manifesting in landslides even in the absence of a geothermal energy development activities. One of the challenges of a geothermal power development will be management of the environmental issues such as landslide.

1.2 The Case for a Business Case for Geothermal Power Plant

Building a business case for a geothermally powered LNG plant in western BC (Figure 3), is meant to add to the existing body of knowledge on the renewable energy opportunity that exist in the region. It is also intended to review geological uncertainties peculiar to the study area. further attentions especially as it may impact the region socially and environmentally. It may also be asked, why bother considering geothermal energy for the region when solar or wind or may be cheaper? The detailed response to that type of presumption is contained in the discussion session of this report, where in the result of comparison of technical capabilities as well as the social and economic dimension of three energy systems were compared. Previous studies have determined the thermal potentials for this area. There exist well data that hydrothermal resources that can be run steam turbine power generators to provide baseload electricity for industries and local communities in the region.

The electricity generation potential of geothermal energy resources lying beneath the crust on the western Canadian volcanic complex has been explored through a series exploratory activities and well geothermal potential testing. Similar to other regions traversed by the Pacific Ring of Fire (Fugue 9), including the Cocos, the Nazca plates, as well as the Philippine Plate, the Canadian volcanic complex situated in the province of British Columbia is home to several volcanic belts, with steep thermal gradients where the $200^{o}C$ isotherm is within 2km of the surface. At the end of 2019, the United States, Mexico, Guatemala, El Salvador, Honduras, Nicaragua, Costa Rica, Panama, Colombia, Ecuador, Peru, Bolivia, Chile, New Zealand, Micronesia, Papua New Guinea, Indonesia, Philippines, China, Japan, and Russia (DiPippo, 2016), have attained a combined geothermal power generation installed capacity of 15,406 MW (Richter, 2020). This project thus depends on these geothermal power plants in assessing the potential for a geothermal power plant in the study area. Consistent with ongoing energy transition activities, this project will estimate gain of greenhouse gases (GHG) emissions reduction from adopting geothermal energy instead of fossil fuel. It is also hoped that this alternative clean energy will provide employment for local communities in the region.

1.3 Project Aims & Objectives

The overarching objective of this project is to contribute to the decarbonization of electricity power generation in BC. I intend to build a case for a geothermal power plant in the Mount Meager Volcanic Complex in BC. This project also seeks to understand why there has been no electricity generation from geothermal energy resources that exist in the region (Figure 3) – what are the technical uncertainties that prevent the development of the geothermal resource in the region. The project also utilized available data to classify the geothermal resource based on relevant global classification standard.

1.4 Decarbonizing Electricity Power Generation

Bernier 2018, explained that decarbonization of electricity system is one of the Pan-Canadian Framework (PCF) strategy on Clean Growth and Climate Change, developed to grow the economy while reducing emissions. The desired state is to attain clean, reliable, and affordable electrification. The 2016 Canadian First Ministers meeting issued the Vancouver Declaration on Clean Growth and Climate Change and agreed that a collaborative approach between provincial, territorial, and federal governments as an important step to reduce GHG emissions and to enable sustainable economic growth. The aim of Vancouver declaration is to Implement GHG mitigation policies in support of meeting or exceeding Canada's 2030 target of a 30% reduction below 2005 levels of emissions. Decarbonization which also means increasing the proportion of non-emitting electricity generation is one big justification for investing geothermal power plant. It is not emitting, uses no fossil fuel and can provide baseload power. It should consider and be brought into the energy mix. This project was conceived to make contribution to the ongoing efforts to understand what it will take to bring about the development of the geothermal resource in a cost-effective manner, to support LNG projects and other industries in BC. The end point for this project is a business case using both economic indicators and consideration for social and environmental benefits.

Chapter 2 - Literature Review

Previous studies have demonstrated potential for geothermal energy resources in British Columbia, Canada. One of the earliest records of geothermal heat flow studies in Canada is found in a report titled “Five measurements of heat flow in southern Canada” by Jessop & Judge (1971), reporting estimated heat flow from a shallow well at Penticton, BC; a location 480 km southeast of the study area. Geothermal energy research by the Government of Canada was initiated as part of a major new approach to the problems of future energy supply, prompted in October 1973 by the sudden rise in the price of oil and the subsequent popular perception that the supply of oil was approaching a serious decline (Jessop, 2008). B.C Hydro became involved in 1974 with reconnaissance geological and geophysical investigation as well as with small-scale diamond drilling project designed to evaluate the thermal characteristic of the Meager Creek Hotsprings and the surrounding area” (BC Hydro & Power Authority, 1985). The BC Hydro’s report recognized Mt. Meager area as having the most geothermal prospects in Canada. The first drilling at the Meager Creek Hot Springs occurred in March 1974, a brief seismic survey was conducted during the winter of 1974-1975, before funds were available for geothermal energy studies (Jessop A., 2008). The period of between 1975 and 1982 had witnessed the drilling 22 exploratory wells with 3 of the wells being deeper that 3000m (Proenza, 2012).

The exploratory activities at Mt. Meager and the surrounding area had seen many players contributing to the development of the body of knowledge regarding the geothermal potential of the region. The potential for geothermal electricity generation in the Mount Meager Volcanic

Belt was a subject of the reports of reconnaissance surveys carried out in the region (Natural Resources Canada, 2019; Lyle, 2019).

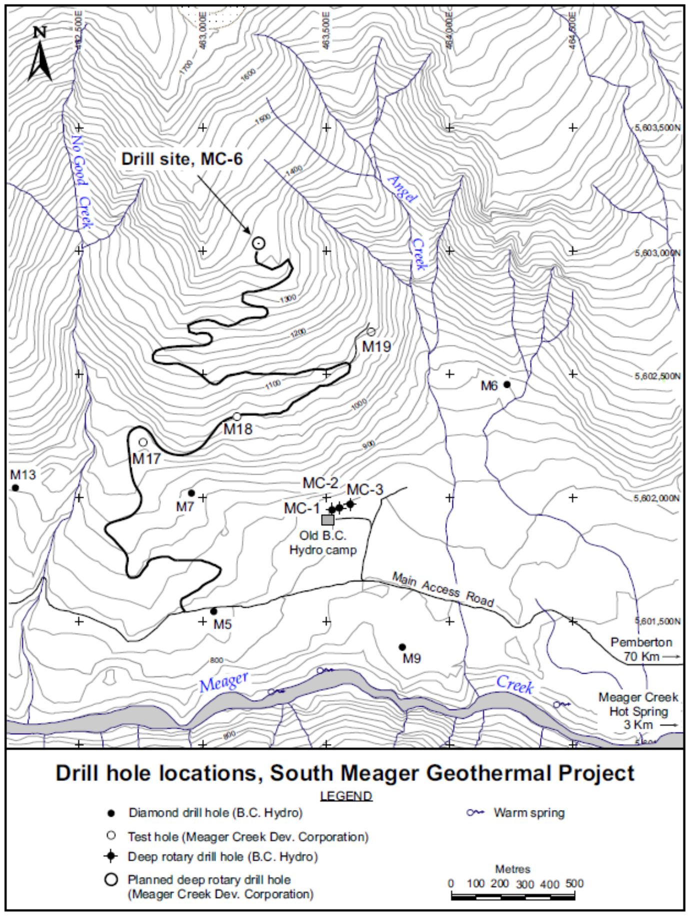

Figure 4: Map of South Mt. Meager geothermal prospective area showing the location of drilled geothermal wells figure from GeothermEx Inc. (2009)

The Geothermal Energy Program of 1974 to 1985 also successfully gathered data upon which subsequent studies were based. However, the project was inconclusive on predicting economic viability of a geothermal plant at that time because flow rates from the drilled holes around Mt. Meager, “were too low to justify the power-transition cost over the distance required” (Grasby et al, 2019). The technical success of the exploration program was limited by the ability to predict the occurrence of permeability at depth (Grasby et al., 2019).

The most recent field work and data gathering project was embarked upon in the summer of 2019. The intention of that study was to gather scientific data that can provide information to predict permeability at depth. (Grasby & Salas (2020) reported how novel geophysical tools and techniques - passive seismic activities, measurements of natural magnetic and electric fields, were used to obtained new data. Detail findings from the analysis of new data collected during the field work is expected to address some of the crucial subsurface uncertainties.

2.1 Key Concepts

2.1.1 Geothermal Energy

Geothermal energy is thermal energy generated and stored in the Earth. It is a renewable energy source that is extracted from fluid and vapor that are naturally heated within the earth's crust. "Deep geothermal energy is one of the few renewable energy sources that is constantly available" (Warren, 2018).

DiPippo, 2016 argued that there are five features that are essential to making a hydrothermal (i.e., hot water/steam) geothermal resource commercially viable. They are:

1. A large heat sources
2. A permeable reservoir
3. A supply of water

4. An overlying layer of impervious rock
5. A reliable recharge mechanism.

A highly schematic depiction of such a system is shown in Figure 5 and DiPippo, 2016 wrote about it as follows:

> "Cold recharge water is seen arriving as rain (point A) and percolating through faults and fractures deep into the formation where it comes in contact with heated rocks. The permeable layer offers a path of lower resistance (point B) and as the liquid heats it becomes less dense and tends to rise within the formation. If it encounters a major fault (point C) it will ascend toward the surface, losing pressure as it rises until it reaches the boiling point for its temperature (point D). There it flashes into steam which emerges as a fumarole, a hot spring, a mud pot or a steam-heated pool (point E)". (p. 10-11)

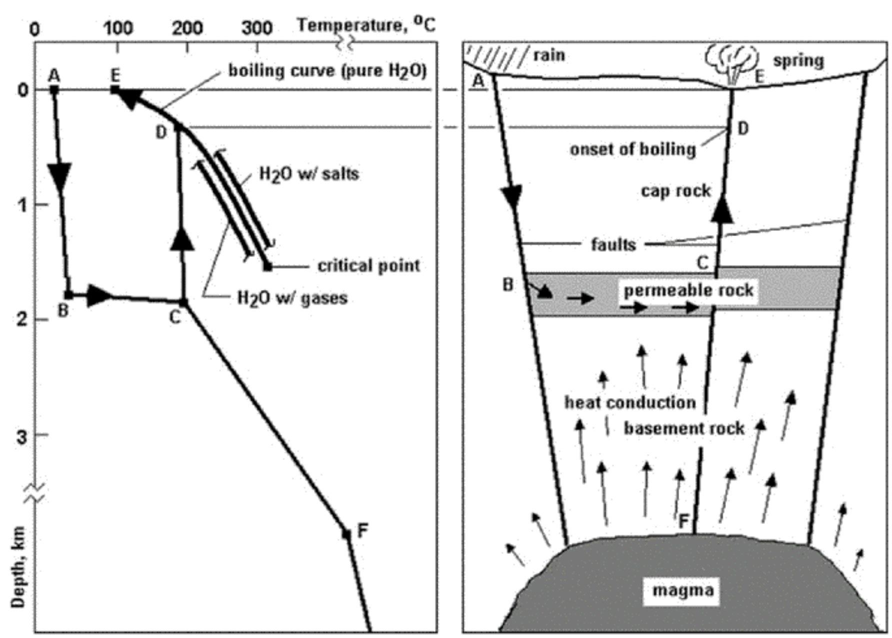

Figure 5: Schematic model of a hydrothermal geothermal system (DiPippo, 2016)

2.1.2 The Active Geothermal Regions

In an effort to maintain a uniform size and shape, our planet Earth has adopted a series of extension and compression of the lithospheric plates as it has been moved around by the convective current of the magma in the Earth mantle. USGS, 2001 explains that most of the movement occurs along narrow zones between plates where the results of plate-tectonic forces are most evident.

According to USGS 2001, there are four types of plate boundaries:

- Divergent boundaries: where new crust is generated as the plates pull away from each other.
- Convergent boundaries: where crust is destroyed as one plate dives under another.
- Transform boundaries: where crust is neither produced nor destroyed as the plates slide horizontally past each other.
- Plate boundary zones: broad belts in which boundaries are not well defined and the effects of plate interaction are unclear

The volcanic country, Iceland is splitting along the spreading center between the North American and Eurasian Plates, as North America moves westward relative to Eurasia. This explains the high geothermal resource potential for Iceland. Iceland’s geothermal energy produces a total installed electricity power capacity of 755 MW (Richter, 2020), which amount to 25% of the country's total electricity production (Orkustofnun National Energy Authority, 2020). In addition, geothermal energy meets the heating and hot water requirements of around 90% of the nation´s housing (Haraldsson, 2014).

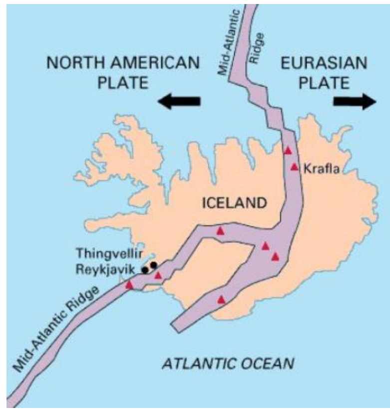

Figure 6: Map showing the Mid-Atlantic Ridge splitting Iceland and separating the North American and Eurasian Plates. Map adapted from U.S. Geological Survey

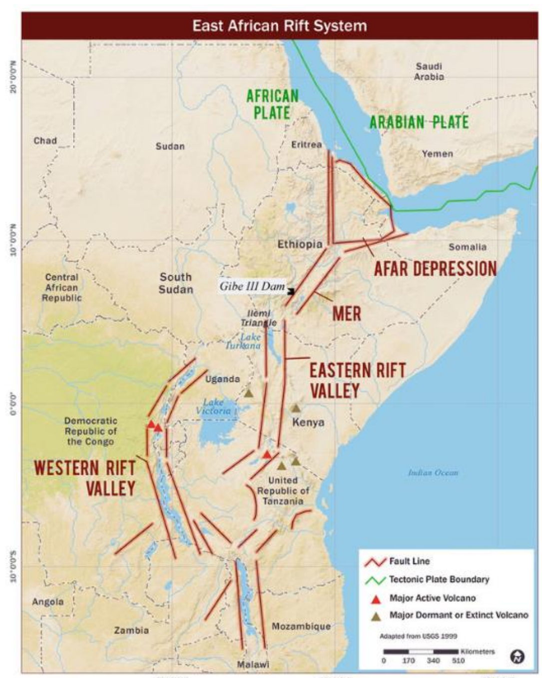

Figure 7: The East Africa Rift System with Main Ethiopian Rift (MER). Map adapted from U.S. Geological Survey

The East Africa Rift System is another example of a divergent plate boundary. "Geothermal resources in Kenya are located within the Rift Valley with an estimated potential of between 7,000 MW to 10,000 MW spread over 14 prospective sites" (Energy & Petroleum Regulatory Authority, Kenya, 2020).

An example of a transform boundaries is the San Andreas Fault (Figure 8) as well as parts of the Juan de Fuca oceanic place which is subducted under the continental North America plate. The Mount Meager Volcanic Complex is associated with volcanic activities related to this convergence plate system and it "lies in the Garibaldi volcanic belt and is the northernmost volcano of the Cascade arc that extends to northern California" (Smithsonia Institution - NMNI, 2013)

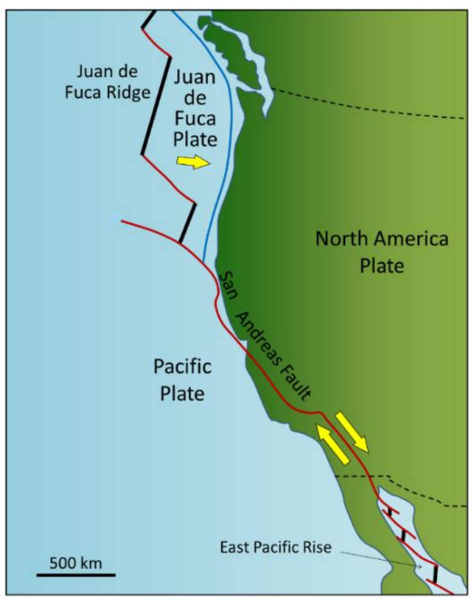

Figure 8: The San Andreas Fault extends from the north end of the East Pacific Rise in the Gulf of California to the southern end of the Juan de Fuca Ridge. All the red lines on this map are transform faults (Earle, 2015).

2.1.3 Global geothermal power generation capacity

Global geothermal power generation capacity stood at 15,406 MW at the year-end 2019 (Richter, 2020). From the viewpoint of geothermal exploitation, the most important of these occur along the edges of the gigantic Pacific Plate, the so-called “Pacific Ring of Fire.” If we include the two adjacent eastern plates, the Cocos and the Nazca plates, as well as the western one, the Philippine Plate, then the following countries are affected United States, Mexico, Guatemala, El Salvador, Honduras, Nicaragua, Costa Rica, Panama, Colombia, Ecuador, Peru, Bolivia, Chile, New Zealand, Micronesia, Papua New Guinea, Indonesia, Philippines, China, Japan, and Russia (DiPippo, 2016, p. 9). All these countries have exploitable geothermal resources and 13 of them have geothermal power plants in operation as of December 2014 (DiPippo, 2016). Subduction zones exist beneath all land masses in contact with the Pacific, Cocos, and Nazca plates, except the contiguous United States and Mexico where transform boundaries exist. “The Alaskan Aleutian Islands lie in a subduction zone and Hawaii lies over a localized hot spot in the middle of the Pacific Plate” (DiPippo, 2016).

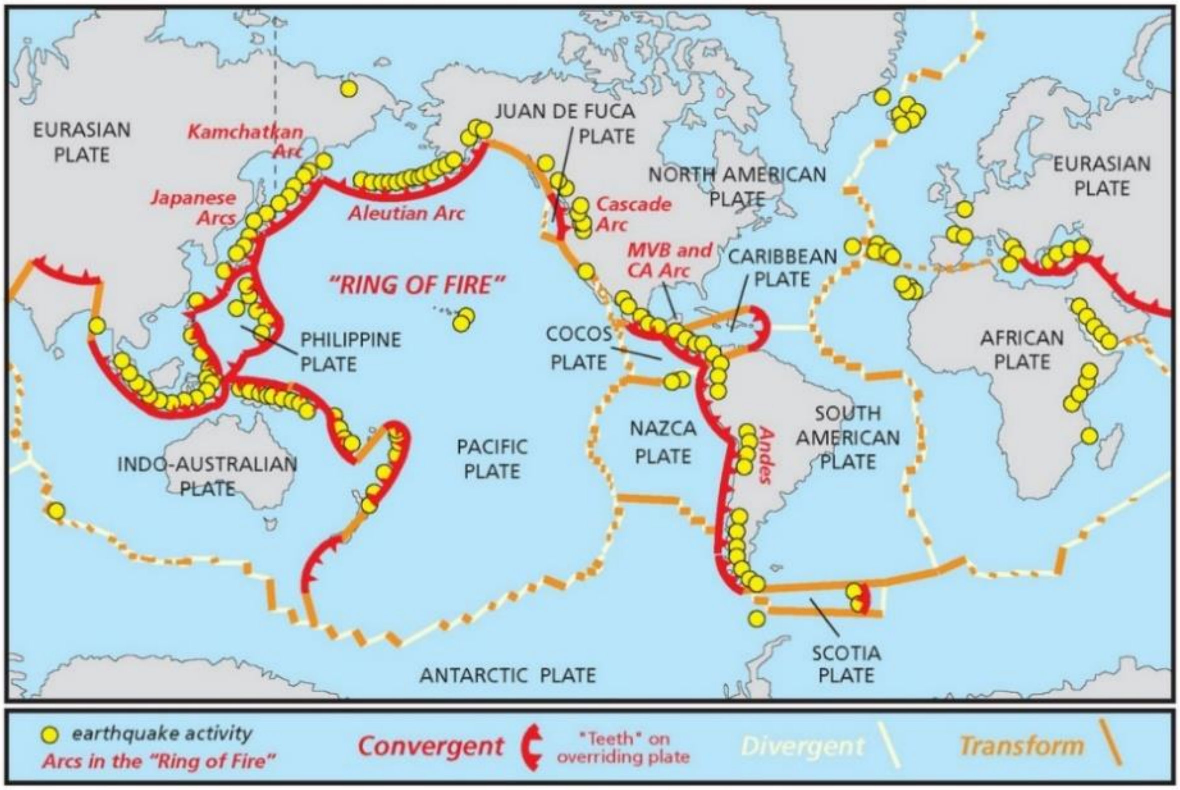

Figure 9: Pacific "Ring of Fire" illustrated in the world map (obtained from "Sendai Japanese Earthquake" website)

2.2 BC Geothermal Exploration Background

Since 1987, with the Brundtland commission's "Common Future", there has been a growing concern about environmental problems in our planet. The combustion of fossil fuel has been recognized as the main cause of climate change which if not curbed can increase the severity of extreme weather conditions and can potentially impact global economy and human society adversely. Anthropogenic GHG emission has been attributed to the climate change that we world witness today. Climate change has been seen to manifest in terms of changes in the ocean circulation, migration of animal, insect and plant species, and some melting of polar icecaps and subsequent rise in sea level. Geothermal energy being of the sources of energy that has near zero environmental impact is been considered globally a viable alternative that can be developed to provide baseload electricity supply that can fill the gap fossil fuel may leave behind.

Despite two decades of scientific research on geothermal in Canada, no geothermal electricity power generation from geothermal and that is not unconnected to the immature stage of the required technical basis. According to Geoscience BC, 2020, if geothermal energy resources are to play a significant role in the future Canadian economy, reliable, baseline geoscience information about the depth, temperature and permeability of potential aquifers – and their suitability to generate geothermal heat and power – is necessary. “To address this issue, a new research project was initiated to help reduce exploration risk for geothermal energy associated with volcanic systems, with a focus on the Garibaldi volcanic belt” (Geoscience BC, 2020).

In the spring of 2020, researchers from the Geological Survey of Canada plus 7 Universities presented preliminary report on outcome of the field work that as carried out during the summer of 2019. Grasby, et al. (2019) discussed how novel geophysical tools and techniques were used to obtained new data. The new data includes measurement of passive seismic activities, measurement of natural magnetic and electric fields that move through the earth to provide 3D insight into the physical nature of geothermal reservoirs that underlies the Mt. Meager area. Detail findings from the analysis of the data collected during the field work is expected to address some of the remaining technical uncertainties.

Chapter 3 - Method of Analysis

I propose, in respect to the study area, that the economic viability of the geothermal resource development is linked to the uncertainties that the hydrothermal resources (i.e. steam or hot water) exist within the plutonic rock of the Mount Meager Volcanic Complex (MMVC), and that it is recoverable in sufficient quantity (i.e. high mass flow rate) and at high temperature (i.e. high geothermal gradient) to produce electricity energy that will pay back the investment with a positive net present value (NPV). The initial assumption is that MMVC meets the requirements for a geothermal system which "includes a source of heat at depth, a large volume of permeable rock, the presence of deep circulating fluids with potential for recharge and the surficial cap of impermeable rocks in order to contain the system's heat" (Proenza, 2012). More than 22000 m of drilling was completed between 1974 and 1982 (Proenza, 2012) and data collected from these wells were used in this study. Well MC-1 was flow tested and connected to a flash steam turbine with a name plate capacity of 20KW, which was tested up to 30KW output (BC Hydro & Power Authority, 1985). This report however mentioned flow limitation that may be due to insufficient rock permeability and suggested further studies and consideration of some other turbine technology such as binary or multi-flash cycle which were not well developed in the 1980s.

3.1 Well Data & 3D Model

Well data were downloaded from Geoscience BC website and loaded for 3D visual analysis using Schlumberger Petrel. The Meager creek fault was digitized from reports and fitted into the model to provide qualitative visual illustration of structural realization. This was done in a deterministic manner based on inferences drawn from available literatures and represents the best interpretation of the authors. This representation is a simple conceptual model; however, it enables a qualitative analysis of the subsurface uncertainties.

The temperature model was built using geothermal gradient data from 15 wells. A high thermal gradient is observed at approximately 1000m below the surface on the north of meager creek fault part of the field; the area penetrated by well MC-6, MC-7, and MC-8. There is an extensive zone of high temperatures over 200°C which is sufficient to produce high enthalpy hydrothermal resources (i.e. steam and hot water). This geothermal reservoir is composed of heterogeneous, fractured quartz diorite basement host rock in 1200 –1600 m depth range and bounded by three major faults in the west, south and east. The model is consistent with geothermal data analysis results (Proenza, 2012).

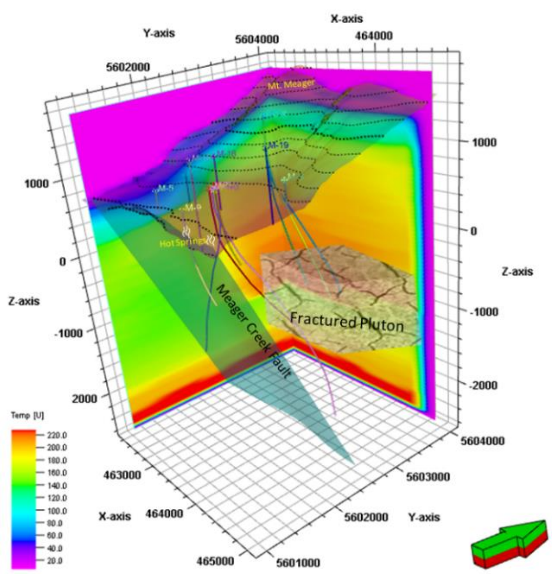

Figure 10: 3D visualization of the geothermal prospect of the plutonic Mt. Meager Volcanic Complex

3.2 Modelling Geothermal Heat Transfer

Numerical modeling of the heat transfer within a single well was modeled as a cylindrical conduit as shown in Figure 4, which represents the well casing, lined with steel with a thermal conductivity "k" (16.3 W/mK @ 100ºC) and surrounded by the formation (quartz diorite) with a thermal conductivity of k = 2.4W/mK.

Also, we conceive a flow of water, m, from one end of the pipe with temperature T_{b1} to the other T_{b2} for a small interval of length L and diameter d along the well. The description of all parameters considered in the numerical analysis of the conceptual flow system model is given in Table 1 below.

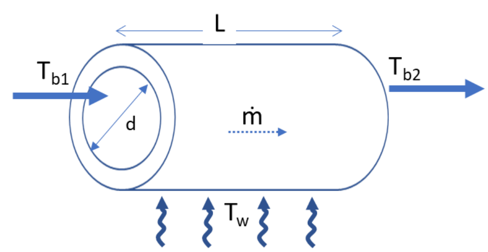

Figure 11: Cylindrical model that forms the basis of the numerical analysis

The amount of heat released by the rock into the flowing water can be represented by the equation Q = mC_pΔT, where Q is the heat energy transferred (in joules), ṁ is the mass flow rate in [kg/s] is a measurement of the amount of water flowing; Cp is the specific heat capacity of the liquid [kJ/kg/°C], and ΔT is the change in temperature of the liquid (degrees Celsius).

Given the well dimensions and temperature gradient, it is possible to derive the outlet water/steam temperature, T_{b2}, and mass flow rate (ṁ)

$$q = h\pi dL\left(T_w - \frac{T_{b1}+T_{b2}}{2}\right) = \dot{m}C_p(T_{b2} - T_{b1}) \quad (1)$$

$$h = \frac{kNu_d}{d} \quad (2)$$

The Nusselt number is a dimensionless number which gives the ratio between convection heat transfer & conduction heat transfer. Nusselt number is required to find 'h' which is the convective heat transfer coefficient (Holman, 2010).

$$Nu_d = 1.86(Re_d.Pr)^{\frac{1}{3}}\left(\frac{d}{L}\right)^{\frac{1}{3}}\left(\frac{\mu}{\mu_w}\right)^{0.14} \quad (3)$$

Equation 3 is a somewhat simpler empirical relation for laminar (Holman, 2010). In this formula the average heat-transfer coefficient is based on the arithmetic average of the inlet and outlet temperature differences, and all fluid properties are evaluated at the mean bulk temperature of the fluid, except μ_w, which is evaluated at the wall temperature. Equation eq. 3 obviously cannot be used for extremely long tubes since it would yield a zero heat-transfer coefficient (Holman, 2010), hence the limit of the ΔL.

The Reynolds number (Re_d) is a dimensionless quantity in fluid mechanics used to help predict flow patterns in different fluid flow situations (Holman, 2010) and is defined as:

Reynolds Number (Re_d) = Inertial Force / Viscous Force

$$Re_d = \frac{\rho.u_m.d}{\mu} \quad (4)$$

The Prandtl Number "Pr" is a dimensionless number approximating the ratio of momentum diffusivity (kinematic viscosity) to thermal diffusivity and is defined as (Holman, 2010).

$$\mathrm{Pr} = \frac{\mu\, cp}{k} \qquad (5)$$

where μ, cp and k are defined in Table 1 below.

For laminar flow, water Mass Flow Rate ($\dot{m}$) is thus given by:

$$\dot{m} = \rho \frac{\pi d^2}{2} u_m \qquad (6)$$

Three critical parameters required for the sizing of the steam turbine are the outlet temperature, the mass flow rate (kg/s) and the pressure (kPa). Table 1 itemizes all the parameters of interest and excel rendering of the model in illustrated in Appendix A.

Table 1: List of parameters for the numerical analysis

Parameter	Notation	Unit
Depth	D	m
Pipe Diameter	d	m
Mean Flow velocity	u_m	m/s
Pipe Section Length	L	m
Constant Wall Temperature	Tw	^oC
Water Inlet Temperature	Tb1	^oC
Water Outlet Temperature	Tb2	^oC
Water Density	ρ	kg/m^3
Water Viscosity @ Mean Bulk Temperature	μ	kg/m.s
Water Thermal Conductivity	k	W/m.C
Water Specific Heat Capacity	cp	J/kgK
Prandt Number	Pr	
Reynolds Number	Re_d	

Water Viscosity @ Wall Temperature	μ_w	kg/m.s

(Adepoju, 2020)

3.3 Simulated Flow Scenarios

Three scenarios are analyzed to represent the finite flow possibilities considering variable permeability. Scenario 1 (Figure 12) illustrate fluids circulation enable by induced permeability with imparted fractures in the plutonic rock. This concept can be implemented to support fluid injection and re-injection for a guaranteed stabled flow rate. The second and third scenarios illustrated in Figure 13 and 14 respectively, are similar to the "EAVOR-Loop" configuration. These three scenarios are used to study the impact of variable well surface area on heat transfer within the aquifer and flow rate.

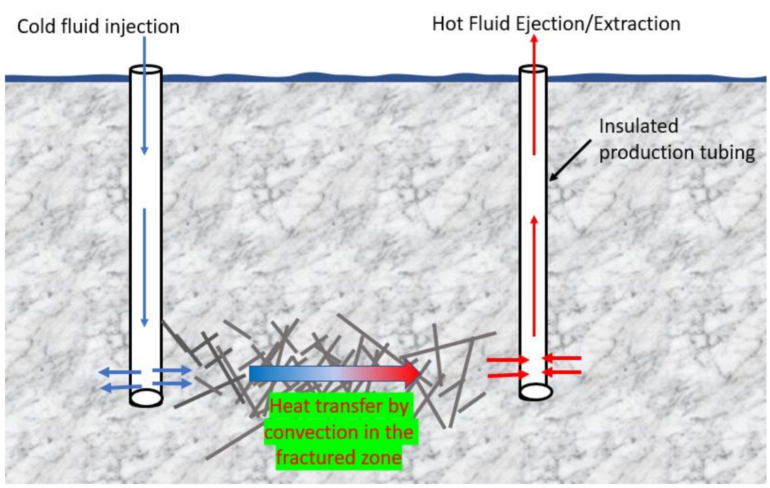

Figure 12: Scenario 1 -Conventional vertical (or deviated) well targets the sufficiently fractured and permeable zone.

A possible injection well can be installed at some time in the future or simultaneously

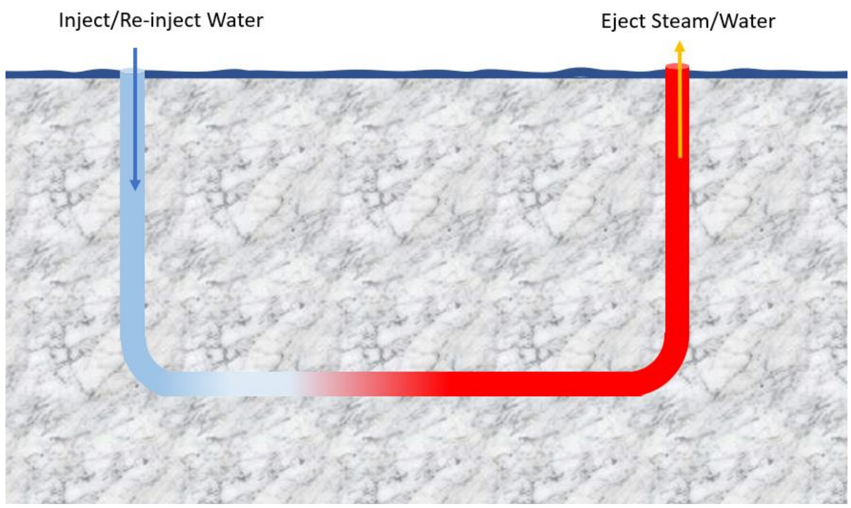

Figure 13: Scenario 2 – Lateral loop well configuration.

The basement rock is not sufficiently naturally fractured and induced fracturing is avoided for environmental reasons.

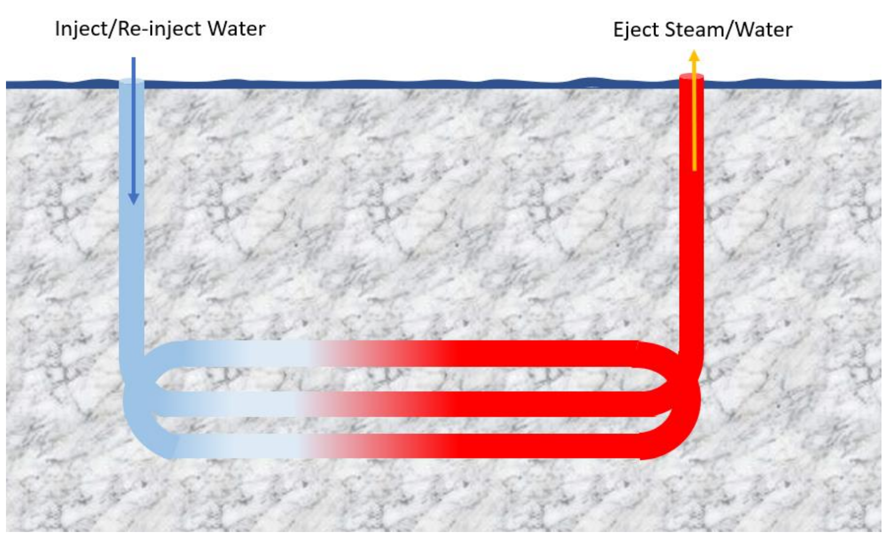

Figure 14: Scenario 3- Multi-laterally loop well configuration.

The basement rock is not sufficiently naturally fractured and induced fracturing is avoided for environmental reasons. Multilateral legs to ensure high contact surface area to geothermal heat source.

3.4 Analysis of Rock Property

Porosity of the rock was estimated using equation (6)

$$\Phi_{fr} = 0.001 A_{fr} D_{fr} F_{fr} \tag{6}$$

Equation (6) is based on fracture permeability equations attributed to Dr Zoltan Barlai (Crain, 2019), where Φ_{fr} = fracture porosity (fractional), A_{fr} = fracture aperture (mm), D_{fr} = number of main fracture directions (1 for sub-horizontal or sub-vertical & 2 for orthogonal sub-vertical), F_{fr} = fracture frequency (fractures per meter). Permeability is the property of rocks that is an indication of the ability for fluids (gas or liquid) to flow through rocks. High permeability will allow fluids to move rapidly through rocks. In this study, our permeability (K_{fr}) estimate was based on empirical analysis of permeability of fractured rocks in pressurized volcanic and geothermal systems represented with equation (7) (Lamur, et al., 2017).

$$K_{fr} = 6x10^{-13}\, \Phi^{0.64} \tag{7}$$

where $\Phi = \Phi_{fr}$,

3.5 Cost Analysis

Current geothermal drilling technology has evolved from a combination of oil and gas and hydrothermal drilling practices due to similarity of equipment and materials. (Lukawski a, et al., 2014). According to the US Department of Energy, Office of Energy Efficiency and Renewable

Energy, the initial costs for the field and construction of a geothermal plant in the US is roughly $2500 per installed kW. This cost estimate is exclusive of the drilling and completion cost and assumed at $4000 per meter obtained from interviews and benchmarked with Lukawski, et al. (2014) geothermal well cost equation (8).

$$Cost\ of\ geothermal\ well = 1.72\ x10^{-7}MD^{2} + 2.3x10^{-3}\ \mathrm{MD} - 0.62 \qquad (8)$$

where "MD" is measured depth, or the total length of the well.

3.6 Resource Classification

To classify the resource, we adopt the United Nations Framework Classification for Resources update 2019. "The United Nations Framework Classification for Resources (UNFC) is a resource project-based and principles-based classification system for defining the environmental-socio-economic viability and technical feasibility of projects to develop resources. UNFC provides a consistent framework to describe the level of confidence of the future quantities produced by the project" (United Nations, 2020).

3.7 Financial & cost estimate assumptions

RetScreen calculates the energy (electricity) production cost per kWh (or MWh). This value (also called the Levelized Cost of Electricity or LCOE) represents the electricity export rate required in order to have a Net Present Value (NPV) equal to 0. The GHG reduction revenue, the customer premium income (rebate), the Other revenue (cost) and the Clean Energy (CE) production revenue are not included in this calculation. The assume value is $0.1032/kWh

3.8 Capacity Factors

The capacity factor, which represents the ratio of the average power produced by the power plant over a year to its rated power capacity (CF). The value assumed in this modeling was based on the data from the US DOE for Geothermal plants that operate in the US as benchmark. The DOE capacity factor database for geothermal power plants is referred to as collated from the mix of power plants serving the electricity grid. Same US DOE database was also considered as a guide along other available capacity factor data for the wind turbine and solar PV systems. The Solar CF assumption used for RetScreen models (Table 2), were based on the environmental conditions as provided for by the RetScreen application which marches the Canada Energy Regulator's database (Figure 17).

Where geothermal power plants can be operated as base load, the capacity factor is usually more than 0.9. (Stefánsson, 2002). However, the more conservative option was taken (Table 2). Below therefore is the table of the capacity factors that was assumed for this project.

Table 2: Capacity factor table for Geothermal, Wind Turbines and solar PV utility grade system

	Geothermal	**Solar**	**Wind**
Capacity Factor (ei.gov) US database	72.23%	23.54%	33.07%
Capacity Factor (Stefánsson, 2002)	90%	-	-
Capacity Factor (RetScreen database)	90%	11%	20 to 40%
Capacity Factor (average from Warren, 2018)	92.37%		
Capacity Factor (Canada Energy Regulator) data for BC		12% - 15.5%	
CANWEA (data for BC)	-	-	34%
Capacity Factor assumption for the project	**75%**	**12%**	**35%**

(Adepoju, 2020)

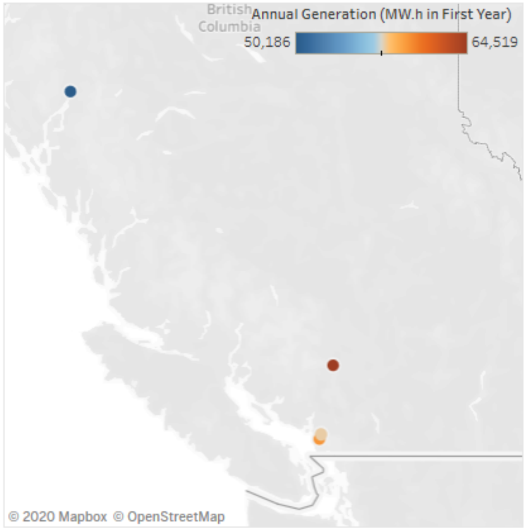

Annual Generation by Community and Province or Territory

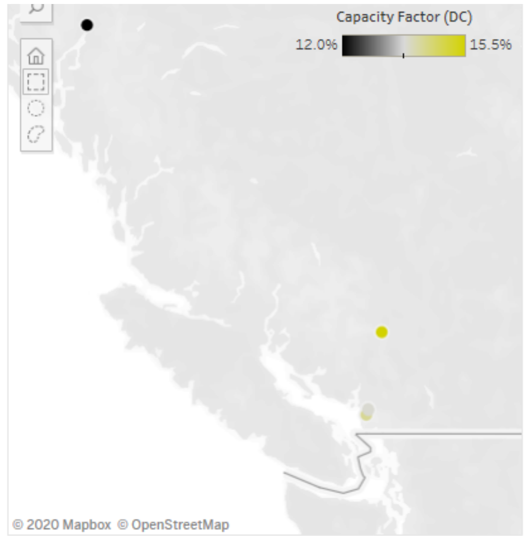

Capacity Factors by Community and Province Or Territory

Figure 15: Capacity Factor map obtained from Canada Energy Regulator, 2019

Chapter 4 - Discussion

4.1 Impact of rock property

Permeability has an exponential relationship with fracture aperture in fractured reservoir (Figure 16). Lamur et al, (2017) had noted that a relative increase in permeability of up to four orders of magnitude can occur when fractures are imparted on rocks.

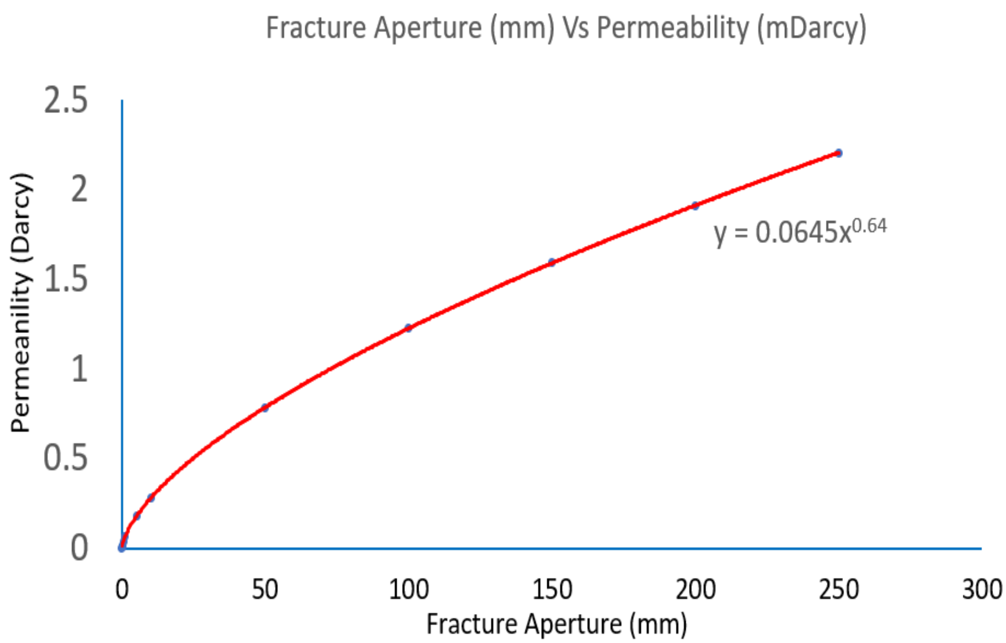

Figure 16: An exponential relationship between fracture Aperture and permeability.

We also observed a non-linear relationship between mass flow rate and rock permeability represented by variable drill-hole dimension in the model (Figure 17)

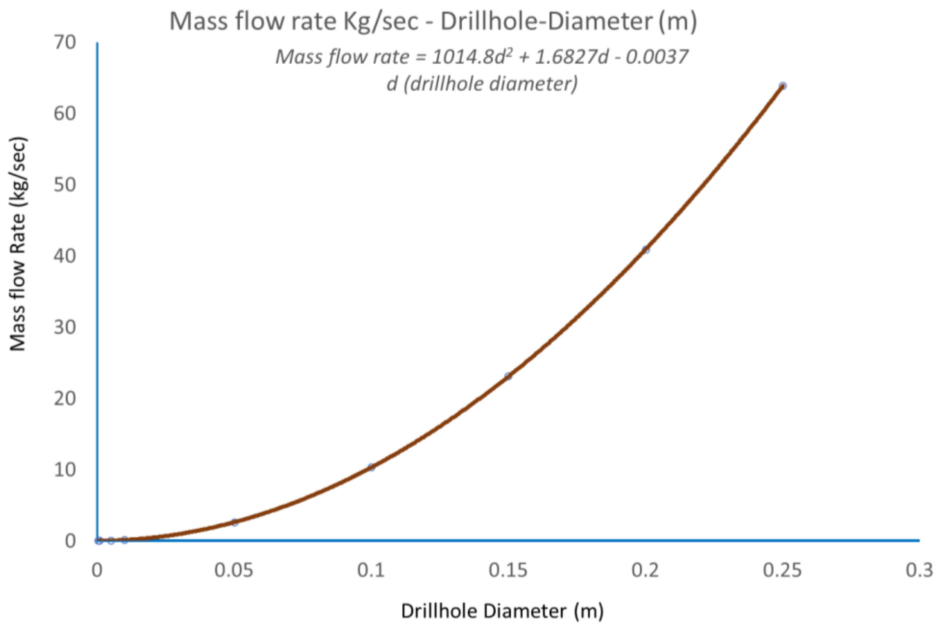

Figure 17: A non-linear relationship between mass flow rate and rock permeability

The hydrothermal resource mass flow rate relates lineally to fluid injection rate (Figure 10). However, a rapid fluid injection will limit rate of heat transfer (Figure 9), therefore a reasonable balance is required to achieve hydrothermal mass flow rate, pressure and outlet temperature that will be optimal for an economically viable geothermal power plant. This observation is common across the three conceptual flow models that was tested. The conventional or enhanced geothermal system as represented in scenario 1 (Figure 12) provides the biggest opportunity for geothermal exploitation in the study area.

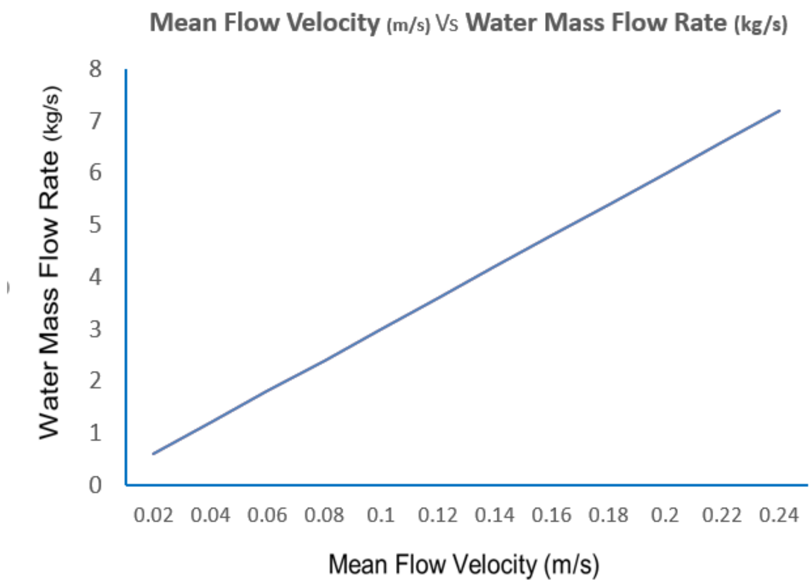

Figure 18: Flow velocity is proportional to mass flow rate.

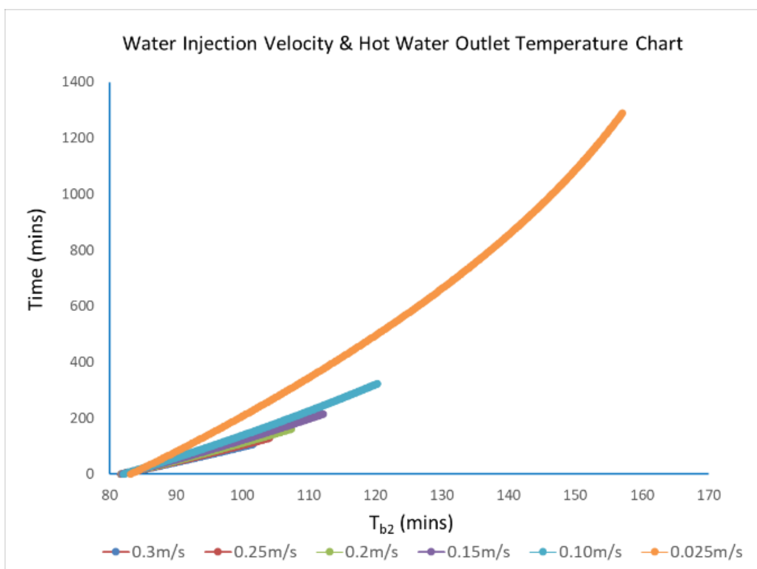

Figure 19: For a 2km loop, low flow velocity favors high outlet temperature, but low mass flow rate as illustrated in Figure 17

The conventional well design targeting either the naturally fractured zones of the geothermal sweets spot promises hydrothermal resources would be more hot water based rather than vapor dominated. Benchmarking using White and William chart (Figure 20), suggests that the loop scenarios falls below reasonable steam power generation threshold and only the conventional wells drilled into a permeable plutonic rock is capable of globally comparable power generation for the study area.

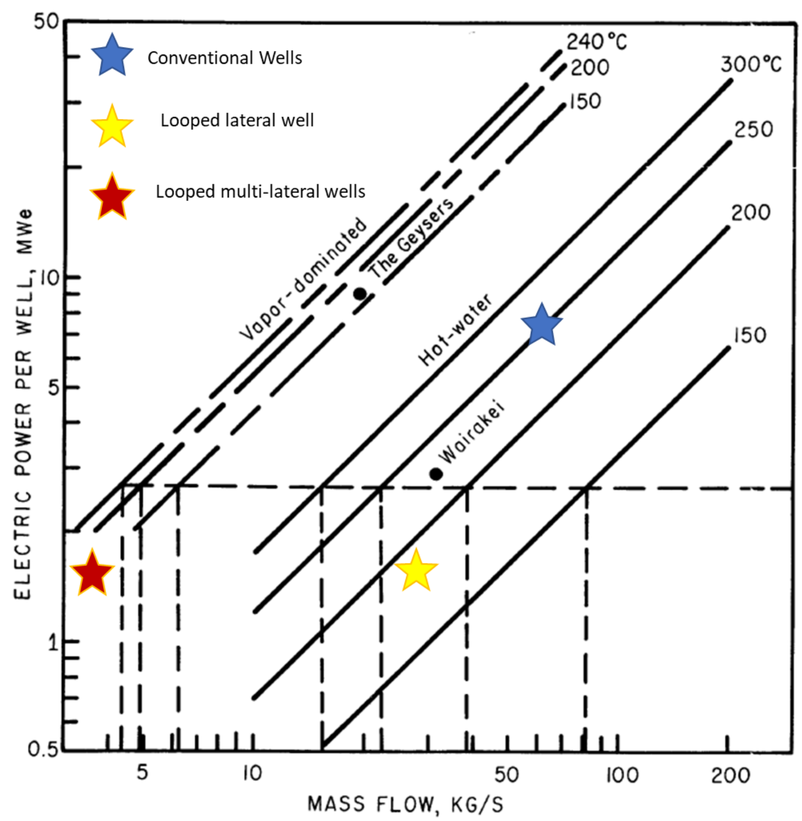

Figure 20: Electric power per well as a function of mass flow for various temperatures of hot water -and vapor-dominated systems, modified from (White & Williams, 1975).

Looped flow scenarios illustrated in Figures 12 and 13 do not support a combination of high mass flow rate and hot enough water that favors positive economics when compared with the convectional EGS. Also, in terms of the initial implementation cost, the multilateral configuration turned out to have the most negative net present value (Figure 21), whereas the conventional EGS well configuration (scenario 1) is most returns a positive NPV considering a 30 years facility life cycle and considering similar financial premise.

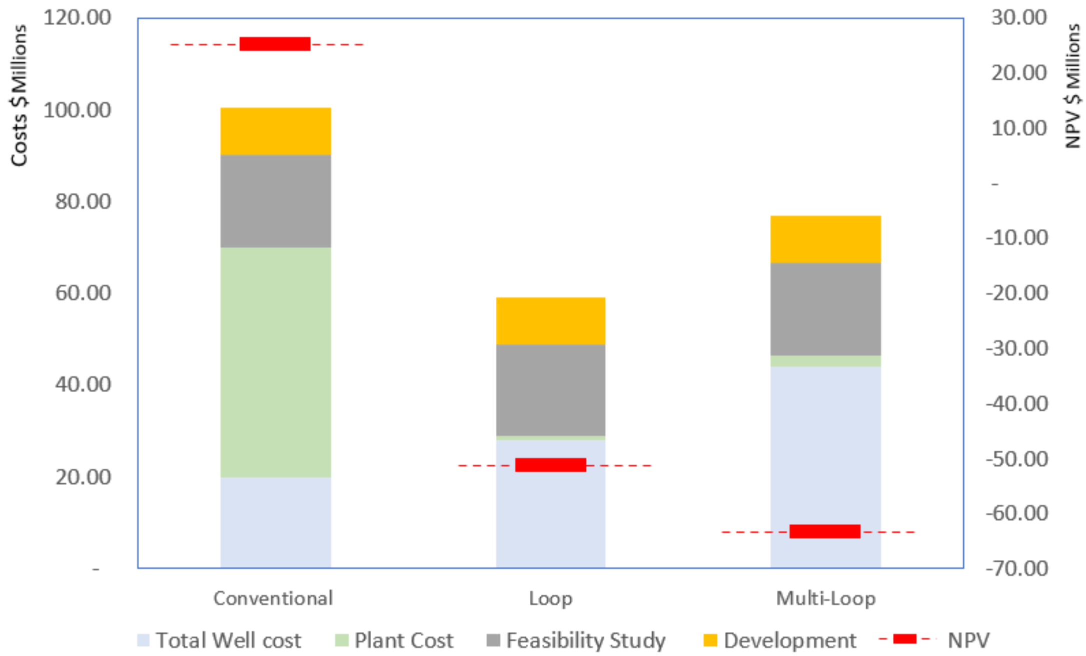

Figure 21: Cost of geothermal plant with well and the actual surface plant facility is presented

Sensitivity on rock permeability (Figure 22), using flow rate as proxy suggests that a flow rate below 40kg/sec will amount to a negative net present value (NPV) and it reflected also in the extended simple payback period which is the time it would take to recover the initial investment in energy savings (Figure 23)

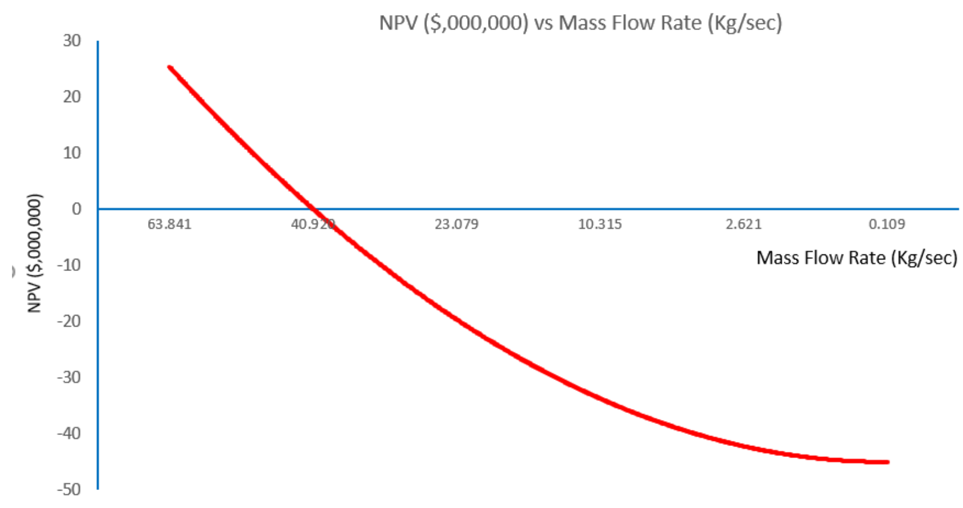

Figure 22: NPV vs mass flow rate chart

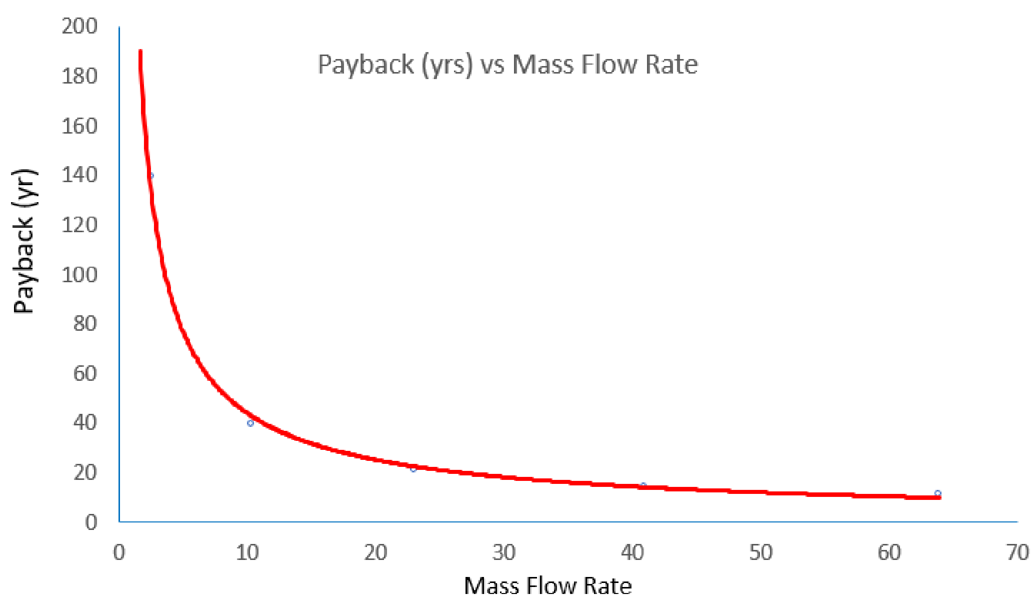

Figure 23: Payback vs mass flow rate chart

Sensitivity analysis as illustrated on the Tornado chart in Figure 24, suggests that permeability uncertainty impacts geothermal power plant economics more that geothermal gradient uncertainty does. It is therefore recommended further research to de-risk the permeability of the MMVC geothermal aquifer. It is also recommended to implement enhanced geothermal system (EGS) to harvest the geothermal resource when it becomes clear that development of the geothermal resource is economically feasible in this area. We recognize that EGS may have environmental implication that may be related to the risk of landslide in the region. High-volume injection for a short period near a critically stressed fault can induce long-lasting seismicity (Ogwari, DeShon, & Hornbach, 2018).

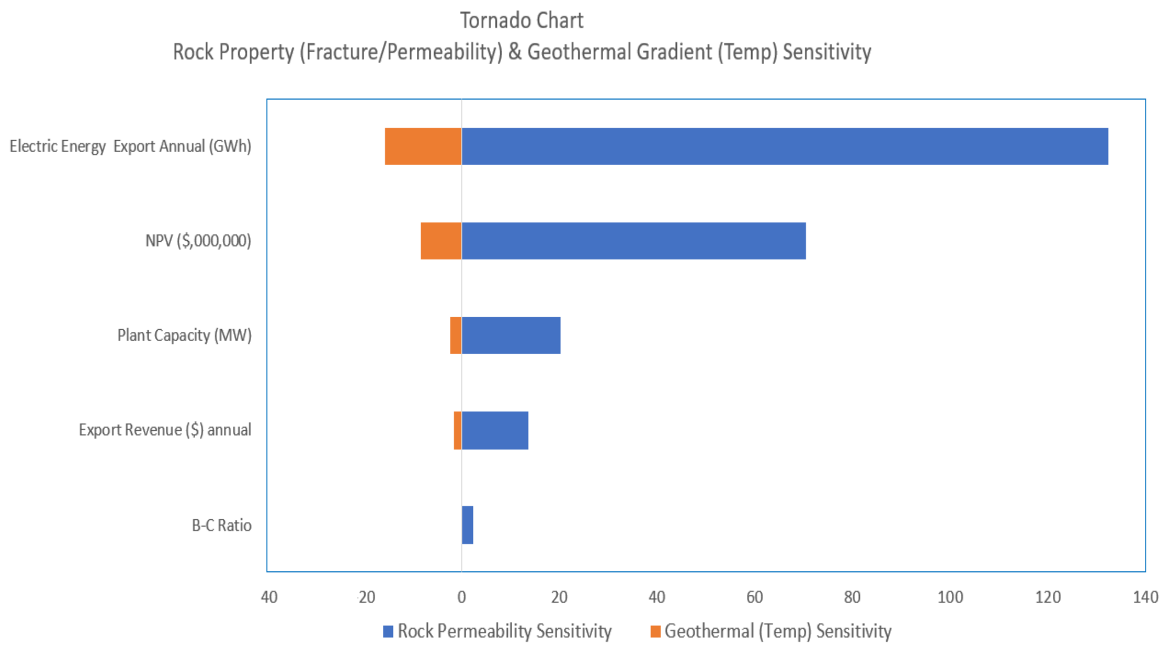

Figure 24: Tornado Chart illustrating sensitivity of permeability and geothermal gradient on economics of geothermal power plant.

Table 3: Comparison of Energy Resources: Geothermal, Solar and Wind Energies.

Parameter Description	Solar	Geothermal	Wind
Capacity (MW)	20.1	20.1	21
Capacity Factor	12.10%	75%	35%

Electricity exported to grid (MWh)	21,380.09	132,381.11	64,386.00
Electricity export revenue	1,924,208	13,661,730.81	6,644,635.20
O&M	211,916.25	4,633,338.94	1,575,000.00
Initial cost	29,342,250.00	100,746,660.95	52,500,000.00
Total cost	29,342,250.00	100,746,660.95	52,500,000.00
Pre-tax IRR -equity	6.41%	13.01	14.07
Pre-tax IRR- assets	2.32%	6.67	7.3
Simple payback	16.90	11.00	10.21
Equity payback	17.84	8.80	8.05
NPV ($)	- 4,506,960.49	25,219,058.62	16,644,981.24
Annual life cycle savings ($/yr)	- 438,691.09	2,454,731.15	1,620,161.74
Cost Benefit (B-C) ratio	0.69	1.50	1.63
GHG reduction credit ($/tCO2)	20	20	20
Debt service coverage	1.3848	2.1318	2.2595
GHG reduction revenue	24,031.22	148,796.37	72,369.86
GHG reduction credit duration	30	30	30
GHG reduction credit escalation rate	3%	3%	3%
Net annual GHG emission reduction (tCO2)	1,201.56	7,439.82	3,618.49

(Adepoju, 2020)

The business case is being presented using following parameter

1. Comparison of the net present value of investments in the three energy systems
2. Comparing the payback times of the investments in the three energy systems
3. Comparing the Internal rate of return (IRR) of the of investments in the three energy systems
4. Capex will be considered in terms of ease of financing along with the benefit-cost ration for the investments.
5. GHG reduction potential and Annual life cycle savings for each energy systems.

Even though the models for each power system was built with a capacity of 20MW, the units were capped or controlled by various capacity factors, which are dictated by the weather for both Solar and Wind. In the case of Geothermal, the weather is not determinant for capacity factor. Geothermal capacity factor can be high as over 90% if the plant is operated as base load. The energy source is from the earth and not controlled by weather, rather by the operator. Figure 25 illustrates the relationship between the capacity factor and the electricity exported to the grid. Solar being the lowest capacity factor exported lest. Geothermal having the capacity factor (≈75%), can export 132,381.11MWh.

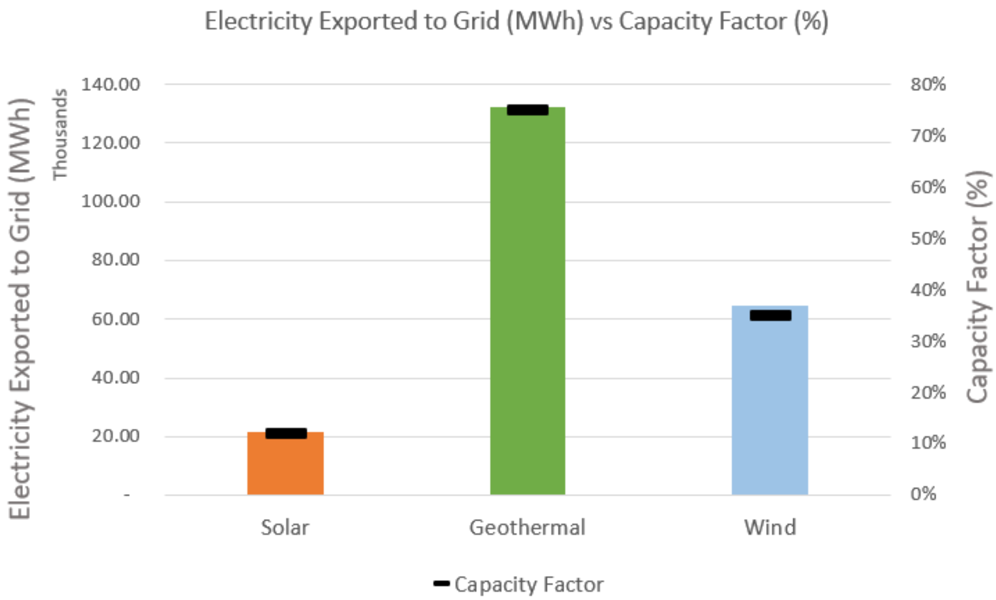

Figure 25: A plot of electricity generation and capacity factors for geothermal plant, wind turbine and solar PV systems.

The model calculates the Net Present Value (NPV) of the project, which is the value of all future cash flows, discounted at the discount rate of 9% across the three models. Under the NPV method, the present value of all cash inflows is compared against the present value of all cash outflows associated with an investment project. The difference between the present value of these cash flows, called the NPV, determines whether the project is generally a financially acceptable investment or not. Positive NPV values are an indicator of a potentially feasible project.

Geothermal has the highest CAPEX and the most positive net present value (NPV), while solar PV system has a negative NPV. Wind turbines maintained a medium profile (Figure 24). Also, in terms of payback, Geothermal performs well relative to the others, far better than solar PV system of similar generation capacity of (≈20MW). A geothermal plant has a CF of 75% has a cost that is double the cost of the wind turbine with same capacity, but it pays back the investment at about same duration as the Wind turbine farm which has a CF of 35%.

The annual life cycle saving was estimated in RetScreen as the levelized nominal yearly savings having the same life and net present value (NPV) as the project. The annual life cycle savings are calculated using the net present value, the discount rate, and the project life. Comparing these energy systems based on the GHG emission reduction and annual life cycle savings, Geothermal savings better (Figure 27). While solar of that scale returns negative (-$438,691.09) saving, Geothermal save $2,454,731.15 while Wind turbine $1,620,161.74.

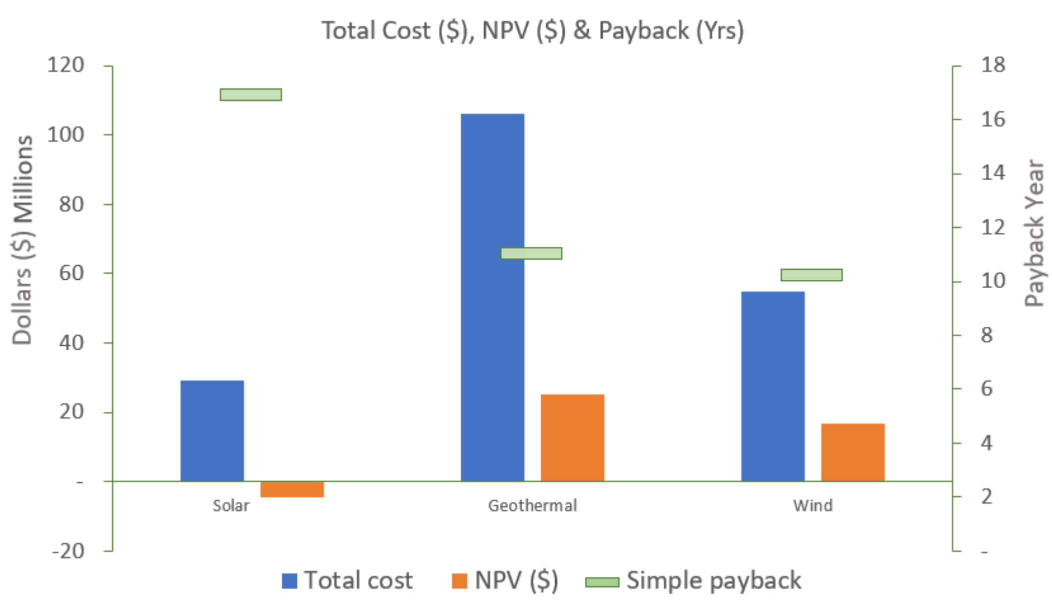

Figure 26 ; CAPEX, NPV and payback chart

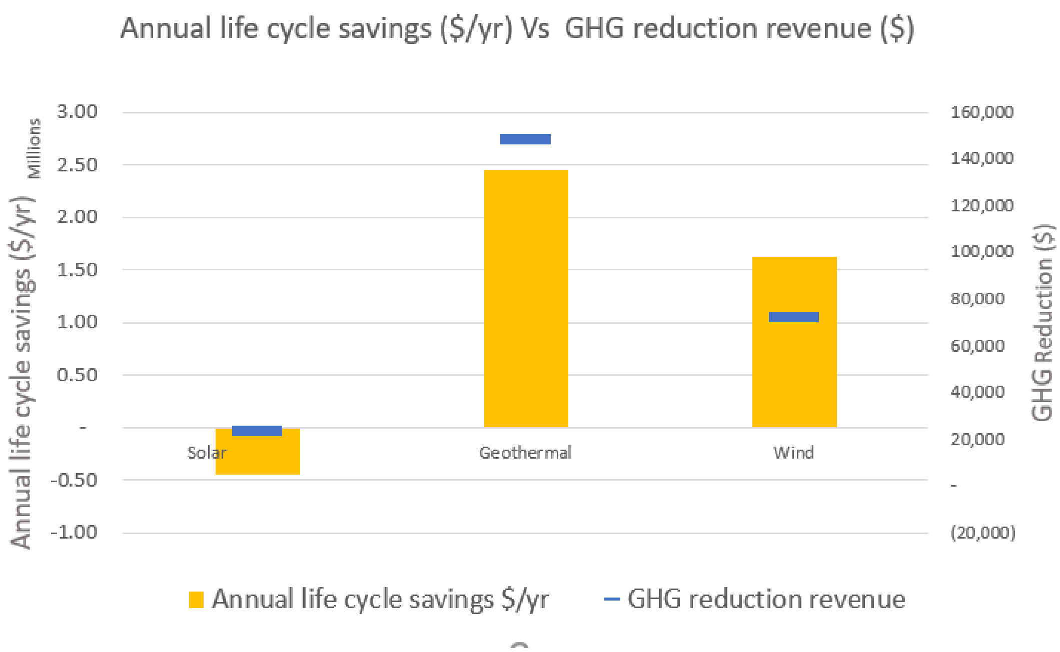

Figure 27:Annual life cycle savings was plot with the GHG reduction revenue to demonstrated that bulk of the saving is related to GHG reductions

Also, the model calculates the net Benefit-Cost (B-C) ratio, which is the ratio of the net benefits to costs of the project. Net benefits represent the present value of annual revenue and savings, while the cost is defined as the project equity. Social and ecological cost is not factored into this estimate. Geothermal and wind energy systems as modeled compares well in this category with ratios greater than 1 (Geothermal 1.91 and Wind 2.09), also indicating profitability. Solar has a B-C ratio of 0.53. The net benefit-cost ratio as a profitability index, leads to the same conclusion as the net present value indicator (Figure 28).

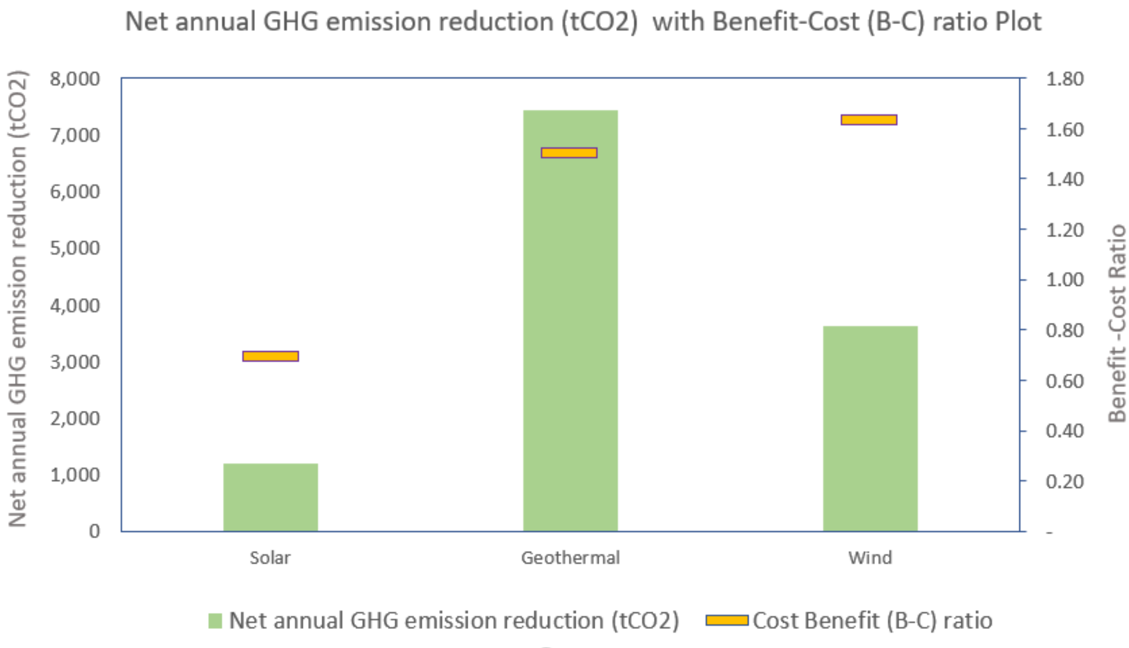

Figure 28: Profitability index plotted with net annual GHG emission reduction.

4.2 Potential Environmental Implications

Landslides are quite prevalent in the area, especially at loosely consolidated volcanic edifices like the Mount Meager Volcanic Complex (MMVC) (Pitchel & Quane, 2019). Alam, 2018's report also published on theglobeandmail.com report volcanilogists as saying that climate change is causing glaciers atop Mount Meager in British Columbia to shrink, increasing the chances of landslides and even a new eruption. "A landslide in 2010 from Mount Meager unleashed about 53 million cubic metres of rock and created a dam on Meager Creek about 300 metres wide and two kilometers long. About 5,000 people downstream were evacuated because of the threat of a rapid release of the lake that formed behind the dam" (Alam, 2018). A collaborative effort under the auspices of the Quest Summer Fellowship Program is helping to create a landslide alarm system to protect power plant that may be located at the base of the MMVC. (Pitchel & Quane, 2019).

There is also a risk of shifting of location geothermal resources that impact of social and economic benefits if something technical goes awfully wrong during geothermal plant implementation. "Drying or disappearance of natural hot springs in the surrounding area, may lead to loss of natural scenery and then loss of tourism economy and subsequent loss of rare thermophilic plants and algal growth" (Kristmannsdo´ttir & Armannsson, 2003). Toxic wastewater entering clean aquifers due to lowering of the water table. (savingiceland.org, 2008). "Violent Hydrothermal (phreatic) explosions caused by buildup of a 'steam pillow' in empty hot underground reservoirs, which have previously killed people working in geothermal plants" (Goff, & Goff, 1997).

4.3 Water Use & Environmental Impact

Re-injection of water can increase water withdrawal and reduce water consumption. Indeed, some of the hydrothermal resources can be consumed while been allocated for secondary economic benefits such as space warming and in pool warming and tourism. Production and injection wells would be designed and constructed with corrosion proof casing materials to prevent cross-contamination with groundwater systems (Clean Energy BC, 2020).

Water injection and reinjection may also induce microseismicity that can increase the chance of land instability. "Given enough time, the pressure increase created by injection can migrate substantial horizontal and vertical distances from the injection location. Induced earthquakes can occur 10 or more miles from injection wells. Induced earthquakes can also occur a few miles below injection wells" (USGS, Are earthquakes induced by fluid-injection activities always located close to the point of injection?, n.d.), High-volume injection for a short time period near a critically stressed fault can induce long-lasting seismicity (Ogwari, DeShon, & Hornbach, 2018). There are also risk of air and chemical pollution with toxic elements (Kristmannsdo´ttir & Armannsson, 2003).

While wind turbine might be an acceptable investment financially, it may not suit this location for stability issues. Unlike in offshore wind turbine farm and that of prairie or flat land wind farm, mountain wind farm has a lot of going against it. The stability of the terrane, lower wind velocity in the region and extreme weather condition that can render the wind turbine inoperable for most of the year.

4.4 Land Use & Environmental Impact

Land impacts also are minimal. Geothermal power plants are typically constructed at or near the geothermal reservoir – there is no need to transport 'fuel' to the plant – and require only a few acres for the plant buildings. Geothermal plants generally have a low profile. Geothermal wells and pipelines may cover a considerable area but do not prohibit other uses such as farming, livestock or wildlife grazing and recreational activities. (Clean Energy BC, 2020)

4.5 Social and Economic benefit

Clean Energy BC estimated that the construction of generating plant, substations, transmission line and other facilities could employ some 250–350 personnel over a two-year construction period. And that once in operation, these facilities would employ some 30–40 persons full-time. Work related to road and transmission route maintenance and similar services would be sub-contracted locally, with employment varying on a seasonal basis. Hot spring spa resort businesses can take advantage of byproduct hydrothermal resources, (hot water not re-injected) to heat pools and spaces in a sustainable way. Indeed, that may require separate investment in water treatment. There are potential for this and the geothermal plant to result in employment for local hand mostly the proximal indigenous communities in the region. Other application can be in agriculture for heating greenhouse, aquaponics and in fishery, all of which could potentially improve the economy and the social wellbeing of the proximal local communities.

4.6 Environmental & Regulatory Considerations

Geothermal projects in BC are subject to the Geothermal Resources Act and Regulations; and to a full range of provincial licensing and permitting requirements covering land leases, drilling permits, wildlife protection, public health and safety, environmental monitoring and protection, road construction and water use. "Power projects with more than 50 megawatts capacity are subject to review under the BC Environmental Assessment Act and Canadian Environmental Assessment Act" (Clean Energy BC, 2020).

4.7 Resource Classification

Geothermal resources at Mt Meager Volcanic Complex falls into the "Potentially Viable Project, E2-F2(F2.1)-G3, Development Pending" class, of the United Nations Framework Classification for Resources (Table 4). This classification standard allows for a direct comparison of projects that extract primary energy fuels, such as oil, gas, coal, and uranium, with renewable energy projects.

The development of new types of resources, such as renewable energy, unconventional petroleum and mineral resources and anthropogenic resources, demonstrates that the historical boundaries between the energy and raw material sectors is no longer valid. Hence, we need to push the adoption of this classification in Canada. It is gradually gaining relevance on the global scale especially for financial reporting, Policy formulation in energy and raw material studies, National resources management functions and Corporate business processes.

UNFC has been adopted as the basis of national resource classification in many countries including China, India, Mexico, Poland, and Ukraine. African Union Commission has decided to develop a UNFC-based African Mineral and Energy Resources Classification and Management System (UNFC-AMREC) as a unifying system for Africa. Development of AMREC includes preparing a Pan-African Resources Reporting Code (PARC). European Commission is assessing the use of UNFC to classify and report raw material resources of Europe.

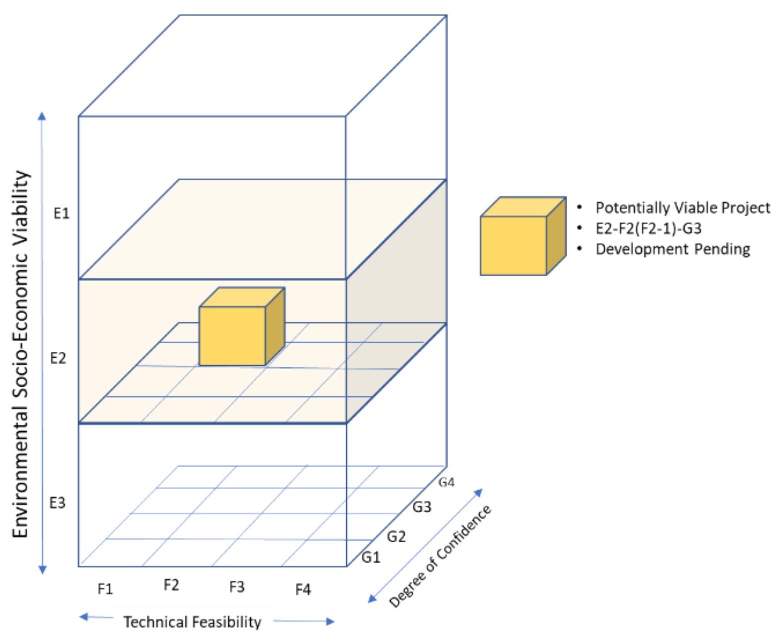

Figure 29: Classification is based on the United Nations Framework Classification for Resources Update 2019

Table 4: UNFC basis for MMVC geothermal resources.

UNFC Category	UNFC Category Definition	UNFC Sub-Category	UNFC Sub-Category Definition
E 2	Development and operation are not yet confirmed to be environmentally-socially-economically viable but, on the basis of realistic assumptions of future conditions, there are reasonable prospects for environmental-socio-economic viability in the foreseeable future.	N/A	
F 2	Preliminary studies of a defined project provide sufficient evidence of the potential for development and that further study is warranted. Further data acquisition and/or studies may be required to confirm the feasibility of development.	F2.1	Project activities are ongoing to justify development in the foreseeable future.
G3	Product quantity associated with a project that can be estimated with a low level of confidence (based on this review).		

(Adepoju, 2020)

Chapter 5 - Conclusion

A geothermal power plant located at MMVC region can produce electricity at LCOE of CAD$0.11/kWh despite known risks if we

1. de-risk geological uncertainties with further research
2. mitigate known environmental risks for instance setup of early warning systems
3. develop supportive policies that incents early adopters/developers

Based on the financial criteria; NPV, IRR and B-C ratio, GHG reduction potential and annual life cycle savings, geothermal power plant ranks higher than wind farm except that capital expenditure (CAPEX) that is required for geothermal plant implementation double what is required for wind turbines. The 20MW plant that was powered by two geothermal wells (a production well and an injection well), can be scaled up to 100MW capacity with additional 2 injection wells, 4 production wells, and 4 more 20MW capacity steam turbines/power generators. Also, running the plant for baseload power supply to industries such as the LNG plants on the western coast could scale up the capacity factor above 0.9. An 100MW capacity geothermal plant may generate an annual 660GWh electricity power supply to the grid, and which may amount to annual GHG emission avoidance from of up to 37,000 tCO2 and significant positive social and economic impact in an environmental responsible manner. And this geothermal resources at Mt Meager Volcanic Complex falls into the “Potentially Viable Project, E2-F2(F2.1)-G3, Development Pending” class, of the United Nations Framework Classification for Resources.

5.1 Limitations & Opportunity for further work

The outcome of my project is limited by the time allotted for this project and available data. A more robust estimate could incorporate history matching technique for benchmarking analysis of the permeability of the plutonic rock that lie beneath the surface of the study area. Also, I recognize that further analysis of the potential for geothermal power plant in the study area can be carried out with more accurate result and reduced uncertainties when the full result of 2019 summer field work to be released starting from 2021 are incorporated in a further study.

Future work can focus on establishing a detail cost of power transmission from Mount Meager Volcanic Complex to specific industrial locations within the region. Also, a further study can focus on the environmental hazard mitigation planning to support huge geothermal power plant investment in the Mount Meager Volcanic Complex in BC.

5.2 Appreciations

Many thanks to Dr. Roman Shor, University of Calgary for supervising this project. I also like to give a special acknowledgement and appreciation for the support and guidance received from the Dr. Zhuoheng Chen (Natural Resources Canada/Geological Survey Canada).

References

Alam, H. (2018). *As climate change shrinks glaciers on B.C.'s Mount Meager, the risk of landslide increases.* VANCOUVER: The Canadian Press. Retrieved from https://www.theglobeandmail.com/canada/british-columbia/article-as-climate-change-shrinks-glaciers-on-bcs-mount-meager-the-risk-of/

BC Hydro & Power Authority. (1985). *Meager Creek Resource Characteristics and 20KW wellhead turbine and seperator testing.* Vancouver: BC Hydro.

Bernier, A. (2018, June 14). *Decarbonizing and electrification: a federal perspective*. Retrieved from Natural Resources Canada- Clean Energy BC: https://www.cleanenergybc.org/wp-content/uploads/2015/09/June-2018-Clean-Energy-BC-Andre-Bernier.pdf

Canada Energy Regulator. (2019, October 18). *Economics of Solar Power in Canada – Results*. Retrieved from Government of Canada: https://www.cer-rec.gc.ca/nrg/sttstc/lctrct/rprt/cnmcsfslrpwr/rslts-eng.html

Clean Energy BC. (2020). *Geothermal Power*. Retrieved from Clean Energy BC;: https://www.cleanenergybc.org/about/clean-energy-sectors/geothermal

Crain, E. R. (2019). *Crain's Petrophysical Handbook.* Retrieved from https://www.spec2000.net/15-permfrac.htm

DiPippo, R. (2016). *Geothermal power plants : Principles, applications, case studies and environmental impact.* Knovel.

Earle, S. (2015). *Physical Geology.* Victoria, B.C: BCCampus. Retrieved from https://opentextbc.ca/

Energy & Petroleum Regulatory Authority, Kenya. (2020). *Geothermal*. Retrieved from EPRA: https://renewableenergy.go.ke/technologies/geothermal-energy/

Geoscience BC. (2020). *Garibaldi Geothermal Volcanic Belt Assessment Project*. Retrieved from Geoscience BC: http://www.geosciencebc.com/projects/2018-004/

GeothermEx Inc. (2009). *Summary of the status of the south meager geothermal project british columbia, canada, for western geopower corporation vancouver, bc canada.* Bc: geothermex Inc.

Glave, J., & Moorhouse, J. (2014). *Lock in Jobs, Not Pollution.* British Columbia: Clean Energy Canada at Tides Canada. Retrieved from cleanenergycanada.org/jobsnotpollution

Goff, S. J., & Goff, F. (1997). *Environmental Impacts During Geothermal Development: Some Examples From Central America*. New Energy and Industrial Technology Development Organization (NEDO) for The NEDO International Geothermal Symposium, 1-10.

Grasby, S. E., & Salas, C. (2020, February 25). *Searching for Mount Meager's geothermal heart*. *EOS, 101*. doi:doi.org/10.1029/2020EO140214

Grasby, S. E., Ansari,, S. M., Calahorrano-Di Patre, A., Chen, Z., Craven, J. A., Dettmer, J., . . . Williams-Jone, G. (2019). *Geothermal Resource Potential of the Garibaldi Volcanic Belt, outhwestern British Columbia (Part of NTS 092J).* Geoscience BC Summary of Activities 2019: Energy and Water.

Haraldsson, I. G. (2014). *Economic benefits of geothermal space heating from the perspective of Icelandic consumers*. Short Course VI on Utilization of Low- and Medium-Enthalpy

Geothermal Resources and Financial Aspects of Utilization”, organized by UNU-GTP and LaGeo,. Santa Tecla, El Salvador: UNU-GTP and LaGeo. Retrieved May 18, 2020, from https://orkustofnun.is/gogn/unu-gtp-sc/UNU-GTP-SC-18-45.pdf

Holman, J. P. (2010). *Heat Transfer.* New York: McGraw-Hill.

Jessop, A. (2008). *Review of National Geothermal Energy Program Phase 2 – Geothermal Potential of the Cordillera.* Geological Survey of Canada .

Jessop, A. M., & Judge, A. S. (1971). *Five measurements of heat flow in southern Canada.* Canadian Journal of Earth Science, 8, 711-716.

Kristmannsdo´ttir, H., & Armannsson, H. (2003). *Environmental aspects of geothermal energy untilization.* Geothermix, 451-461. doi:10.1016/S0375-6505(03)00052-X

Lamur, A., Kendrick, J. E., Eggertsson, G. H., Wall, R. J., Ashworth, J. D., & Lavallee, Y. (2017). *The permeability of fractured rocks in pressurised volcanic and geothermal system*. Sci Rep, 7(1). Retrieved from https://ucalgary-primo.hosted.exlibrisgroup.com/permalink/f/1vibdgm/TN_palgrave_j10.1038/s41598-017-05460-4

Lechtenböhmer, S., & Nilsson, L. J. (2016). Chapter 19 - *Sustainable Energy Systems*. In H. Heinrichs, P. Martens, G. Michelsen, & A. Wiek, *Sustainability Science - An Introduction* (p. 231). New York: Springer.

Lukawski a, M. Z., Anderson, B. J., Augustine, C., Capuano, L. E., Beckers, K. F., Livesay , B., & Tester, J. W. (2014). *Cost analysis of oil, gas, and geothermal well drilling*. Journal of Petroleum Science and Engineering, 18, 1-14.

Lyle, A. (2019). *A hot spot for geoscientists: Exploring geothermal energy potential at Mount Meager. Field study probes energy generation potential, volcanic activity, and stability in British Columbia.* Retrieved from https://www.ualberta.ca/science/news/2019/october/geothermal-energy-mount-meager/

Natural Resources Canada. (2018). *Natural Resources Canada Online .* Retrieved from https://www.nrcan.gc.ca/energy/energy-sources-distribution/natural-gas/canadian-lng-projects/5683

Office of Energy Efficiency and Renewable Energy. (n.d.). *Geothermal FAQs*. Retrieved from energy.gov: https://www.energy.gov/eere/geothermal/geothermal-faqs

Ogwari, P., DeShon, H., & Hornbach, M. (2018). The Dallas-Fort Worth Airport Earthquake Sequence: Seismicity Beyond Injection Period. *Journal of Geophysical Research. Solid Earth, 123*(1), 553-563. doi:10.1002/2017JB015003

Orkustofnun National Energy Authority. (2020). *Geothermal*. Retrieved from nea.is: https://nea.is/geothermal/

Pitchel, M., & Quane, S. (2019). *Landslide Detection at the Mount Meager Volcanic Complex.* Squamish, BC: Quest Summer Fellows Program.

Proenza, Y. (2012). *Geothermal Data Compilation and Analysis of Alterra Power's Upper Lillooet Property - Clean Energy CEEN596 Project.* UBC Clean Energy Research Centre (CERC).

Richter, A. (2020, January 27). *The Top 10 Geothermal Countries 2019 – based on installed generation capacity (MWe)*. Retrieved May 18, 2020, from thinkgeoenergy.com: https://www.thinkgeoenergy.com/the-top-10-geothermal-countries-2019-based-on-installed-generation-capacity-mwe/

savingiceland.org. (2008). *Negative aspects of geothermal power generation.* Retrieved from www.savingiceland.org: www.savingiceland.org

Shaffer, B. (2018). *Will LNG Canada increase greenhouse-gas emissions? It's complicated.* macleans.ca. Retrieved from https://www.macleans.ca/

Smithsonia Institution - NMNI. (2013). *Mount Meager Volcanic Complex*. Retrieved from https://volcano.si.edu/volcano.cfm?vn=320180

Stefánsson, V. (2002). *Investment cost for geothermal power plants*. Geothermics*, 31*(2), 263-272. doi:10.1016/S0375-6505(01)00018-9

United Nations. (2020). *United Nations Framework Classification for Resources Update 2019.* Geneva: United Nations.

USGS. (2001). *This Dynamic Earth; the story of plate technics.* Washington, DC: USGS. Retrieved from http://pubs.usgs.gov/publications/text/dynamic.html

USGS. (n.d.). *Are earthquakes induced by fluid-injection activities always located close to the point of injection?* Retrieved June 18, 2020, from usgs.gov - Natural Hazards:

https://www.usgs.gov/faqs/are-earthquakes-induced-fluid-injection-activities-always-located-close-point-injection?qt-news_science_products=0#qt-news_science_products

Wang, T. (2020, April 7). *Worldwide capacity of geothermal energy 2009-2019*. Retrieved from statista.com: https://www.statista.com/statistics/476281/global-capacity-of-geothermal-energy

Warren, J. P. (2018). Chapter 10 - Deep geothermal energ*y. I*n S. Peake, *Renewable Energy* (pp. 489-539). Oxford: Oxford University Press.

White, D. E., & Williams, D. I. (1975). *Assessment of Geothermal Resources of the United States.* Arlington: Geological Survey Circular.

Appendix A

	A	B	C	D	RT	RU	RV	RW	RX	RY	RZ
1					Section	Section	Section	Section	Section	Section	Section
3		Depth	D	m	90	85	80	75	70	65	60
4		Pipe Diameter	d	m	0.25	0.25	0.25	0.25	0.25	0.25	0.25
5		Mean Flow velocity	u_m	m/s	1.5	1.5	1.5	1.5	1.5	1.5	1.5
6		Pipe Section Length	L	m	5	5	5	5	5	5	5
7		Constant Wall Temperature (insulated)	T_w	C	140	140	140	140	140	140	140
9		Water Inlet Temperature	T_{b1}	C	196.95	196.94	196.93	196.92	196.91	196.91	196.90
11		Water Density @ Inlet Temperature	ρ	kg/m3	866.8513079	866.8619851	866.8726604	866.8833336	866.894005	866.9046743	866.9153417
12		Water Viscosity @ Inlet Temperature	μ	kg/m.s	1.452670526	1.452731544	1.452792557	1.452853568	1.452914574	1.452975577	1.453036577
13		Water Thermal Conductivity @ Inlet Temperature	k	W/m.C	0.674779901	0.674785671	0.674791439	0.674797206	0.67480297	0.674808733	0.674814495
14		Water Specific Heat Capacity @ Inlet Temperature	c_p	J/kgK	4272.526541	4272.515475	4272.504414	4272.493357	4272.482305	4272.471257	4272.460214
15		Prandt Number @ Inlet Temperature	Pr		0.966189347	0.966228224	0.966267098	0.966305969	0.966344839	0.966383706	0.96642257
17	$Re_d = \frac{\rho u_m d}{\mu}$	Reynold Number @ Inlet Conditions	Re		223.774	223.767	223.760	223.754	223.747	223.740	223.734
18	$Re_d Pr \frac{d}{L}$	Additional Parameter	Re.Pr.(d/L)		10.8104	10.8105	10.8106	10.8107	10.8108	10.8110	10.8111
20		Water Viscosity @ Wall Temperature	μ_w	kg/m.s	2.009692638	2.009692638	2.009692638	2.009692638	2.009692638	2.009692638	2.009692638
22	$\overline{Nu}_d = 1.86(Re_d Pr)^{1/3}\left(\frac{d}{L}\right)^{1/3}\left(\frac{\mu}{\mu_w}\right)^{0.14}$ [6-10]		Nu_d		3.930	3.930	3.930	3.930	3.930	3.930	3.930
24	$h = \frac{k Nu_d}{d}$	Heat Transfer Co-efficient @ Inlet Conditions	h	W/m2.C	10.6	10.6	10.6	10.6	10.6	10.6	10.6
26	$\dot{m} = \rho \frac{\pi d^2}{4} u_m$	Water Mass Flow Rate	$\dot{m}$	kg/s	63.82719611	63.82798228	63.82876831	63.8295542	63.83033994	63.83112553	63.83191099
29	$q = h\pi dL\left(T_w - \frac{T_{b1}+T_{b2}}{2}\right) = \dot{m}c_p(T_{b2}-T_{b1})$		T_{b2}	C	196.94	196.93	196.92	196.91	196.91	196.90	196.89
31		Water Mean Bulk Temperature	T_{bm}		196.94	196.94	196.93	196.92	196.91	196.90	196.89
33		Water Density @ Mean Bulk Temperature	ρ	kg/m3	866.8566465	866.8673227	866.877997	866.8886693	866.8993396	866.910008	866.9206744
34		Water Viscosity @ Mean Bulk Temperature	μ	kg/m.s	1.452701034	1.45276205	1.452823062	1.45288407	1.452945075	1.453006076	1.453067074
35		Water Thermal Conductivity @ Mean Bulk Temperature	k	W/m.C	0.674782786	0.674788555	0.674794323	0.674800088	0.674805852	0.674811614	0.674817375
36		Water Specific Heat Capacity @ Mean Bulk Temperature	c_p	J/kgK	4272.521008	4272.509944	4272.498885	4272.487831	4272.476781	4272.465735	4272.454695
37		Density @ Mean Bulk Temperature	Pr		0.966208785	0.96624766	0.966286533	0.966325403	0.966364272	0.966403137	0.966442001
38		Water pressure	P-hρ_g	Pa	765086.3759	722590.4766	680093.5287	637595.5327	595096.4886	552596.3969	510095.2579
40	$Re_d = \frac{\rho u_m d}{\mu}$	Reynold Number @ Mean Bulk Conditions	Re		224	224	224	224	224	224	224
41	$Re_d Pr \frac{d}{L}$	Additional Parameter	Re.Pr.(d/L)		10.81	10.81	10.81	10.81	10.81	10.81	10.81
43	$\overline{Nu}_d = 1.86(Re_d Pr)^{1/3}\left(\frac{d}{L}\right)^{1/3}\left(\frac{\mu}{\mu_w}\right)^{0.14}$ [6-10]		Nu_d		3.930	3.930	3.930	3.930	3.930	3.930	3.930
45	$h = \frac{k Nu_d}{d}$	Heat Transfer Co-efficient @ Mean Bulk Conditions	h	W/m2.C	10.6	10.6	10.6	10.6	10.6	10.6	10.6
47	$q = h\pi dL\left(T_w - \frac{T_{b1}+T_{b2}}{2}\right) = \dot{m}c_p(T_{b2}-T_{b1})$		T_{b2}	C	196.94	196.93	196.92	196.91	196.91	196.90	196.89

	B	SA	SB	SC	SD	SE	SF
1		Section	Section	Section	Section	Section	Section
3	Depth	55	50	45	40	35	30
4	Pipe Diameter	0.25	0.25	0.25	0.25	0.25	0.25
5	Mean Flow velocity	1.5	1.5	1.5	1.5	1.5	1.5
6	Pipe Section Length	5	5	5	5	5	5
7	Constant Wall Temperature (insulated)	140	140	140	140	140	140
9	Water Inlet Temperature	196.89	196.88	196.87	196.86	196.85	196.84
11	Water Density @ Inlet Temperature	866.9260071	866.9366706	866.947332	866.9579916	866.9686491	866.9793047
12	Water Viscosity @ Inlet Temperature	1.453097573	1.453158565	1.453219554	1.453280539	1.453341521	1.453402499
13	Water Thermal Conductivity @ Inlet Temperature	0.674820254	0.674826012	0.674831768	0.674837522	0.674843275	0.674849026
14	Water Specific Heat Capacity @ Inlet Temperature	4272.449176	4272.438142	4272.427112	4272.416088	4272.405068	4272.394052
15	Prandt Number @ Inlet Temperature	0.966461433	0.966500293	0.96653915	0.966578006	0.966616858	0.966655709
17	Reynold Number @ Inlet Conditions	223.727	223.720	223.714	223.707	223.701	223.694
18	Additional Parameter	10.8112	10.8113	10.8114	10.8115	10.8116	10.8117
20	Water Viscosity @ Wall Temperature	2.009692638	2.009692638	2.009692638	2.009692638	2.009692638	2.009692638
22		3.930	3.930	3.930	3.930	3.930	3.930
24	Heat Transfer Co-efficient @ Inlet Conditions	10.6	10.6	10.6	10.6	10.6	10.6
26	Water Mass Flow Rate	63.83269629	63.83348145	63.83426647	63.83505134	63.83583607	63.83662065
29		196.88	196.87	196.86	196.85	196.84	196.84
31	Water Mean Bulk Temperature	196.88	196.88	196.87	196.86	196.85	196.84
33	Water Density @ Mean Bulk Temperature	866.9313388	866.9420013	866.9526618	866.9633204	866.9739769	866.9846316
34	Water Viscosity @ Mean Bulk Temperature	1.453128068	1.453189058	1.453250045	1.453311029	1.453372009	1.453432985
35	Water Thermal Conductivity @ Mean Bulk Temperature	0.674823133	0.67482889	0.674834645	0.674840399	0.67484615	0.6748519
36	Water Specific Heat Capacity @ Mean Bulk Temperature	4272.443658	4272.432627	4272.4216	4272.410577	4272.39956	4272.388546
37	Density @ Mean Bulk Temperature	0.966480862	0.966519721	0.966558577	0.966597431	0.966636283	0.966675133
38	Water pressure	467593.0718	425089.8389	382585.5594	340080.2338	297573.8623	255066.4451
40	Reynold Number @ Mean Bulk Conditions	224	224	224	224	224	224
41	Additional Parameter	10.81	10.81	10.81	10.81	10.81	10.81
43		3.930	3.930	3.930	3.930	3.930	3.930
45	Heat Transfer Co-efficient @ Mean Bulk Conditions	10.6	10.6	10.6	10.6	10.6	10.6
47		196.88	196.87	196.86	196.85	196.84	196.84

	B	SG	SH	SI	SJ	SK	SL
1		Section	Section	Section	Section	Section	Section
3	Depth	25	20	15	10	5	1
4	Pipe Diameter	0.25	0.25	0.25	0.25	0.25	0.25
5	Mean Flow velocity	1.5	1.5	1.5	1.5	1.5	1.5
6	Pipe Section Length	5	5	5	5	5	5
7	Constant Wall Temperature (insulated)	140	140	140	140	140	140
9	Water Inlet Temperature	196.84	196.83	196.82	196.81	196.80	196.79
11	Water Density @ Inlet Temperature	866.9899584	867.00061	867.0112598	867.0219075	867.0325533	867.0431971
12	Water Viscosity @ Inlet Temperature	1.453463473	1.453524444	1.453585412	1.453646375	1.453707336	1.453768292
13	Water Thermal Conductivity @ Inlet Temperature	0.674854775	0.674860522	0.674866268	0.674872012	0.674877754	0.674883494
14	Water Specific Heat Capacity @ Inlet Temperature	4272.383041	4272.372035	4272.361033	4272.350035	4272.339043	4272.328055
15	Prandt Number @ Inlet Temperature	0.966694557	0.966733403	0.966772247	0.966811088	0.966849927	0.966888764
17	Reynold Number @ Inlet Conditions	223.687	223.681	223.674	223.667	223.661	223.654
18	Additional Parameter	10.8119	10.8120	10.8121	10.8122	10.8123	10.8124
20	Water Viscosity @ Wall Temperature	2.009692638	2.009692638	2.009692638	2.009692638	2.009692638	2.009692638
22		3.930	3.931	3.931	3.931	3.931	3.931
24	Heat Transfer Co-efficient @ Inlet Conditions	10.6	10.6	10.6	10.6	10.6	10.6
26	Water Mass Flow Rate	63.83740509	63.83818939	63.83897354	63.83975754	63.8405414	63.84132512
29		196.83	196.82	196.81	196.80	196.79	196.78
31	Water Mean Bulk Temperature	196.83	196.82	196.81	196.81	196.80	196.79
33	Water Density @ Mean Bulk Temperature	866.9952842	867.0059349	867.0165836	867.0272304	867.0378752	867.0485181
34	Water Viscosity @ Mean Bulk Temperature	1.453493958	1.453554927	1.453615892	1.453676854	1.453737813	1.453798768
35	Water Thermal Conductivity @ Mean Bulk Temperature	0.674857649	0.674863395	0.67486914	0.674874883	0.674880624	0.674886364
36	Water Specific Heat Capacity @ Mean Bulk Temperature	4272.377538	4272.366533	4272.355534	4272.344539	4272.333548	4272.322563
37	Density @ Mean Bulk Temperature	0.96671398	0.966752824	0.966791667	0.966830507	0.966869345	0.96690818
38	Water pressure	212557.9826	170048.475	127537.9227	85026.32589	42513.68489	8502.84135
40	Reynold Number @ Mean Bulk Conditions	224	224	224	224	224	224
41	Additional Parameter	10.81	10.81	10.81	10.81	10.81	10.81
43		3.930	3.931	3.931	3.931	3.931	3.931
45	Heat Transfer Co-efficient @ Mean Bulk Conditions	10.6	10.6	10.6	10.6	10.6	10.6
47		196.83	196.82	196.81	196.80	196.79	196.78

Figure 30: Heat Transfer Model in MS Excel